Diode-oscillator fiber-amplifier systems: versatile, high-power spectro-temporal control

This research was financially supported by the Dutch Technology Foundation STW (STW-project TTF.5795).

The work was carried out at the Laser Physics and Non-Linear Optics Group at the Faculty of Science and Technology, University of Twente, P.O. Box 217, 7500 AE Enschede, The Netherlands.

ISBN 90-365-2411-3

DIODE-OSCILLATOR FIBER-AMPLIFIER SYSTEMS: VERSATILE, HIGH POWER SPECTRO-TEMPORAL CONTROL

PROEFSCHRIFT

ter verkrijging van
de graad van doctor aan de Universiteit Twente,
op gezag van de rector magnificus,
prof. dr. W.H.M. Zijm,
volgens het besluit van het College voor Promoties
in het openbaar te verdedigen
op woensdag 27 september 2006 om 15.00 uur

door

Balaji Adhimoolam
geboren op 6 Oktober 1975
te Chennai, India

Dit proefschrift is goedgekeurd door
de promotor prof. dr. K.-J. Boller

Publications

Journals

- B. Adhimoolam, M.G. Hekelaar, P. Gross, I.D. Lindsay, K.-J. Boller, *Wavelength-tunable short-pulse diode-laser fiber-amplifier system around* $1.06\mu m$, IEEE Photon. Technol. Lett., **18**, 838– 840, 2006

- B. Adhimoolam, M. E. Klein, C. J. Lee P. Groß, I. D. Lindsay, and K.-J. Boller, *Spectral shaping of a* $10W$ *diode laser-Yb-fiber amplifier system*, Rev. Sci. Instrum., **77**, 093101-1– 093101-4, 2006

- Balaji Adhimoolam, Marvin E. Klein, Ian D. Lindsay, Petra Groß, Chris J. Lee and Klaus-Jochen Boller, *Widely and rapidly tunable semiconductor master oscillator-fiber amplifier around* $1080nm$, submitted for publication in IEEE Photon. Technol. Lett., 2006

- I.D. Lindsay, B. Adhimoolam, P. Gross, M.E. Klein, and K.-J. Boller, 110 *GHz rapid, continuous tuning from an optical parametric oscillator pumped by a fiber-amplified DBR diode laser*, Opt. Express., **13**, 1234 – 1239, 2005

International Conferences

- B. Adhimoolam, M. E. Klein, I. D. Lindsay, P. Groß, and K.-J. Boller, *Widely Tunable Semiconductor Master Oscillator-Fiber Amplifier with* $9\,W$ *Output at* $1080nm$, Optical Amplifiers and their Applications (OAA) Topical Meeting 2006, Whistler, Canada (Optical Society of America, Washington D.C. 2006), Pres. no: OMC6

- P. Groß, B. Adhimoolam, M.E. Klein, I.D. Lindsay, K. Hsu, and K.-J. Boller, 9-*Watt CW Swept-Wavelength Diode-Oscillator Yb-Fiber-Amplifier System*, Conference on Lasers and Electro-Optics 2006, Long beach, California, USA (Optical Society of America, Washington D.C. 2006), Presn no:CFG5-1

- M.G. Hekelaar, B. Adhimoolam, P. Groß, I.D. Lindsay, and K.-J. Boller, *Amplification of short pulses from a mode-locked diode laser in an ytterbium-doped fiber*, Pacific Rim Conference on Lasers and Electro-optics July 2005, Tokyo, Japan (Optical Society of America, Washington D.C. 2005), paper no. CTuI4-1

- I.D. Lindsay, B. Adhimoolam, P. Gross, M.E. Klein, and K.-J. Boller, *Diode-laser-fiber-amplifier pumped optical parametric oscillator with* 110 *GHz rapid, continuous tuning*, Advanced Solid-State Photonics (ASSP) TOPS vol. 98 (Opitcal Society of America, Washington, D.C.), 2005, poster no. Tub19

- P. Gross, I. D. Lindsay, B. Adhimoolam, M. E. Klein, M. Auerbach, P. Wessels, C. Fallnich, K.-J. Boller, *Mid-IR continuous-wave fiber-laser pumped optical parametric oscillators*, Conference on Lasers and Electro-Optics 2004, Long beach, California, USA (Optical Society of America, Washington D.C. 2004), Invited talk, CMI3

National Conferences

- B. Adhimoolam, I.D. Lindsay, M.E.Klein, P. Groß, and K.-J. Boller, *Characterization of a* 12*W diode oscillator fiber amplifier system for 3He optical pumping*, 29e Fall meeting of the section of Atomic Molecular and Optical Physics(AMO), 2004, abstract no. B2

- B. Adhimoolam, M.E.Klein, I.D. Lindsay, P. Groß, and K.-J. Boller, *Wide and rapid-infrared tuning of a semiconductor amplifier based laser with an acousto-optics tunable filter*, 30e Najaarsvergadering van de Sectie Atoom- Molecuul- en Optische Fysica, Nederlandse Natuurkundige Vereniging, 2005, abstract no. A1

- B. Adhimoolam, I.D. Lindsay, P. Groß, M.E.Klein, and K.-J. Boller, 110*GHz rapid, continuous tuning from a diode-laser-fiber-amplifier pumped optical parametric oscillator*, 30e Najaarsvergadering van de Sectie Atoom- Molecuul- en Optische Fysica, Nederlandse Natuurkundige Vereniging, 2005, abstract no. A2

- B. Adhimoolam, M.G. Hekelaar, P. Groß, I.D. Lindsay, and K.-J. Boller, *Fiber-amplification of wavelength-tunable, ultra-short pulses from a mode-locked diode laser around* 1.06 *microns*, 30e Najaarsvergadering van de Sectie Atoom- Molecuul- en Optische Fysica, Nederlandse Natuurkundige Vereniging, 2005, abstract no. A3

Abstract

Widely and rapidly wavelength tunable near-infrared laser sources are of importance for a variety of applications such as Fourier domain optical coherence tomography, optical frequency domain reflectometry and fiber grating array monitors, but also for applications involving optical pumping of gases. Of particular interest is to make such wide and rapid wavelength tuning available in the mid-infrared molecular fingerprint region, where carbon-hydrogen molecules show highly specific and strong vibrational resonances. A promising way to achieve this goal is the efficient non-linear downconversion of the named near-infrared sources with singly resonant optical parametric oscillators (SROs).

The goal of the present work was to develop near-IR laser sources that are suitable for this task, i.e., which provide a sufficiently high power and which have superior wavelength tuning properties compared to the existing near-IR laser systems that have so far been used to operate SROs. This goal has been realized by developing various types of semiconductor diode laser oscillators, optimized for their spectral and tuning properties, in combination with high power fiber amplifiers. In this thesis, we present the experimental investigation of these various master-oscillators and their power amplification in Ytterbium-doped fibers to multi-Watt power levels, well sufficient for the efficient operation of SROs.

The first master-oscillator used is a multi-section distributed Bragg reflector (DBR) diode laser operating at a wavelength of 1080nm and with a narrow spectral bandwidth of 30MHz. Around 35mW output from the diode laser was used to seed two Ytterbium doped fiber amplifiers of lengths 36m and 50m. The self-pulsing of the fiber amplifiers, produced due to non-linear optical effects in the fibers, was suppressed by a weak current modulation of the diode laser, for causing a controlled increase of the diode laser bandwidth. The suppression of self-pulsing in the fiber amplifiers was studied as a function of DBR diode laser parameters such as seeding power and the bandwidth. The shorter of the two fibers was chosen for our further experiments, since it provided a higher stable output power in combination with a narrower bandwidth.

In a further step, these DBR diode lasers were subjected to much stronger modulation, with the goal to provide radiation with various controlled spectral distributions in the GHz-bandwidth range, matching the typical Doppler-broadening of atomic and molecular resonances. For this, a DC

bias was applied to one section of the DBR laser and a current modulation to another section. The latter modulation was applied in different waveforms and generated broadened spectra of selectable shape, such as a Gaussian shape. Subsequent fiber amplification made these spectra available at Watt-levels, which might find applications such as efficient optical pumping of Helium for nuclear magnetic resonance tomography.
The second master oscillator used was a Fabry-Perot diode laser, mounted in an external grating cavity and actively mode-locked by a 1.4GHz modulation of the injection current. The diode laser emits short pulses with a duration of around 30ps with an average power of 15mW, wavelength tunable via the grating from 1040nm to 1085nm. After amplification in an Yb-doped fiber, these temporal and spectral properties become available at power levels above 9 Watt. This radiation is highly suitable for efficient downconversion in short-cavity SROs to provide wavelength-tunable mid-infrared picosecond pulses in an compact design.
The third master-oscillator is based on a semiconductor tapered amplifier mounted in a unidirectional ring cavity, that includes an acousto-optic tunable filter (AOTF) and a solid-state etalon. The AOTF provides a 36nm wide and rapid wavelength tuning around 1080nm, while the etalon reduces the spectral bandwidth of the laser to the sub-GHz level. Tuning is actually performed via controlled, rapid mode hopping and can cover the entire bandwidth of 36nm in millisecond time intervals, while a fine tuning of the oscillation frequencies can be achieved via tilting the etalon. After fiber amplification these spectro-temporal properties are available at powers above 9 Watts, which should be of interest for making these properties available in the mid-infrared, after efficient downcoversion in an SRO.
In conclusion, this work demonstrates the superiority of the diode-fiber master-oscillator power-amplifier (MOPA) system over other near-IR SRO pump sources. Essentially, these MOPA systems combine the high wavelength agility and excellent modulation capabilities of diode oscillators with the high-power capabilities of Yb-doped fibers. It can be thus be expected that such MOPA systems can, in further research on downconversion in SROs, make the interesting spectral and temporal properties of the near-infrared diodes available in the molecular fingerprint region, to enable a wide range of corresponding applications.

Samenvatting

Nabij-infrarood lasers die snel over een breed golflengte bereik kunnen verstemmen, zijn belangrijk bijvoorbeeld bij optische coherente tomografie in het Fourier-domein, reflectrometrie in het optische frequentie-domein en fiber tralie array monitors, maar ook voor toepassingen waarbij gassen optisch gepompt worden. Er is specifieke interesse voor snelle en over een breed golflengte verstembare lasers in het midden-infrarode gebied omdat in dit gebied zich spectrale 'vingerafdrukken' van koolwaterstof moleculen bevinden, die het gevolg zijn van zeer specifieke en sterke trillingsresonanties van de moleculen. Een veelbelovende benadering om midden-infrarode bronnen te maken bestaat uit het efficient, niet-lineair omlaag converteren van de frequentie van de genoemde nabij-infrarode bronnen met een enkelvoudige resonante optische parametrische oscillator (SRO's). Het doel van dit werk was om een nabij-infrarode laser te ontwikkelen die geschikt is voor deze benadering, in andere woorden, een laser met een voldoende hoog vermogen en sterk verbeterde eigenschappen om te verstemmen vergeleken met bestaande oplossingen om SRO's te gebruiken. Dit doel is gerealiseerd door het ontwikkelen van verschillende soorten halfgeleider diodelaser oscillatoren met geoptimaliseerde spectrale- en verstemeigenschappen, in combinatie met hoog vermogen fiber versterkers. In dit proefschrift presenteren we het experimentele onderzoek naar deze verschillende soorten primaire oscillatoren en de bijbehorende versterking in Ytterbium-verrijkte fibers tot vermogensniveaus van een aantal Watt, meer dan genoeg om SRO's optisch mee te pompen.
De eerste primaire oscillator die gebruikt is, bestond uit een uit meerdere secties opgebouwde gedistribueerde Bragg reflector (DBR) laserdiode met een golflengte van 1080nm en een smalle spectrale bandbreedte van 30MHz. Circa 35mW uitgangsvermogen van de laserdiode is gebruikt als ingang voor twee Ytterbium-verrijkte fiber versterkers van respectievelijk 36m en 50m. Het verstorende zelf-pulserende effect van deze fiber versterkers, geproduceerd omdat er niet-lineaire effecten in de fibers kunnen optreden, wordt onderdrukt door een zwakke stroommodulatie van de laserdiode, wat een gecontroleerde lijnverbreding in de laserdiode veroorzaakt. De onderdrukking van het zelf-pulseren in de fiber versterkers is bestudeerd als een functie van de DBR laserdiode parameters zoals het ingangsvermogen van de versterker en de lijnbreedte. De kortere van de twee fibers is gekozen voor de rest van het onderzoek omdat het een hoger stabiel uitgangsver-

mogen leverde met een smallere lijnbreedte.
In een volgende stap zijn deze diodes onderworpen aan een veel sterkere modulatie, met als doel om licht met verschillende, gecontroleerde spectrale distributies in te genereren in het gebied met een GHz-bandbreedte, wat overeenkomt met de typische Doppler verbreding van resonanties op atomair en moleculair niveau. Om dit te bereiken is een gelijkstroom toegepast op een sectie van de DBR laser en is in een andere sectie de stroom gemoduleerd. Deze modulatie kon verschillende golffuncties hebben, en dit gegenereerde verbrede spectra waarvan de vorm gekozen kon worden, bijvoorbeeld een Gaussische vorm. Door de erop volgende versterking in de fiber werden deze spectra versterkt tot het niveau van enkele Watt's, en dit zou voor toepassingen zoals efficient optisch pompen van Helium voor nucleaire magnetische resonantie tomografie gebruikt kunnen worden.
De tweede primaire oscillator die gebruikt is, was een Fabry-Perot laserdiode, opgesteld in een externe resonator met een tralie en actief ge-modelocked door een 1.4GHz modulatie van de stroom. De laserdiode levert korte pulsen met een tijdsduur van 30ps met een gemiddeld uitgangsvermogen van 15mW, golflengte verstembaar via het tralie van 1040nm tot 1085nm. Na versterking door de Yb-verrijkte versterker deze eigenschappen uit het spectrale- en het tijdsdomein beschikbaar op vermogens niveaus van meer dan 9 Watt. Dit licht is zeer geschikt voor efficient omlaagconversie in SRO's met een korte resonator lengte om golflengte-verstembaar midden-infrarood picoseconde pulsen te leveren in een compact ontwerp.
De derde primaire oscillator is gebaseerd op een geleidelijk smaller gemaakte halfgeleider versterker opgesteld in een eenrichtings ringresonator, dat ook een akoestisch-optische verstembaar filter (AOTF) en een vaste-stof etalon bevat. De AOTF levert een 36nm brede en snelle golflengte verstemming rond 1080nm. terwijl het etalon de lijnbreedte van de laser reduceert tot het sub-GHz niveau. Verstemming is gerealiseerd via het gecontroleerd en snel van resonator-mode verspringen van de laser en kan over het hele 36nm aflopen in milliseconde tijdsintervallen, terwijl voor fijninstelling van de oscillatiefrequenties het etalon gekanteld kan worden. Na versterking door de fiber versterker, waarbij het spectrale en temporele gedrag bewaard blijft, is dit licht beschikbaar op vermogensniveaus van boven de 9 Watt, wat van belang is om efficiente omlaagconversie in een SRO te bereiken.
Samengevat laat dit werk de superioriteit van een diode-fiber primaire oscillator vermogensversterker (MOPA) systeem zien boven andere nabij infra-

rood SRO-pomp bronnen. In essentie combineren deze MOPA systemen de grote golflengte verstelbaarheid en zeer goede modulatie eigenschappen van diode oscillatoren met het vermogen van Yb-verrijkte versterkers om hoge uitgangsvermogens te leveren. Het kan daarom verwacht worden dat deze MOPA systemen, in verder onderzoek naar SRO's de interessante spectrale en temporele eigenschappen van nabij-infrarood laserdiodes beschikbaar maken in het spectrale gebied waar de moleculaire 'vingerafdrukken' zich bevinden, en hiermee een groot aantal applicaties mogelijk maken.

Acknowledgments

I am greatly indebted to my promoter Prof Dr. Klaus-Jochen Boller, who through his constant support, encouragement and often-brilliant ideas guided me during the course of this research. Dr. Ian Lindsay and Dr. Marvin Klein, both have been of immense help, guiding and offering solutions whenever I stumbled through these four years. I always admire and will cherish the patience, understanding and the ability to come up with quick solutions for the various technical problems, shown by all three of you during the countless meetings held during my time here.
I am grateful to Dr. Petra Gross, who assisted me throughout these four years with her invaluable advice and suggestions over many aspects - starting right from my experiments to all the administrative formalities associated with a PhD degree. I also thank Dr. Chris Lee who aided me during my experiments and offered many helpful suggestions on the various articles written during the past one year. I also cherished the company of Ir. M.G. Hekelaar in the lab, and really enjoyed working together with him. I am grateful to Peter van Voorst for readily helping me with the Dutch abstract.
As a fellow PhD student, I would like to mention the contribution of the other Laser Physics PhD students in making these four years highly enjoyable and pleasant. I would like to thank Isabel de la Fuente Valentin, Denny Mathew, Lars Casper, Liviu Prodan, Peter van Voorst, Anton Azarov, Denis Deriga, Arie Irman, Ab Nieuwenhuis, Rolf Loch and Willem Beeker. I greatly appreciated the time spent at lunch with Dr. Petra Gross, Dr. Ian Lindsay, Dr. Chris Lee, Isabel de la Fuente Valentin, Denny Mathew, Lars Casper and Claudia Ruygrok. I will always cherish the time spent in the company of Isabel de la Fuente at the coffee table everyday, with conversation extending over a wide spectrum of issues.
I also would like to thank all other staff members and colleagues of the Laser Physics group and NCLR B.V. Prof. Dr. Fred Bijkerk, Dr. Peter van der Slot, Dr. Piet Peters, Dr. Bert Bastiaens, Dr. Fred van Goor, Dr. Jeroen Verschuur, Dr. Arsen Khachatryan, Huub van Heel, Jacob Couperus, Leon Raanhuis, Simone ter Hedde-Sloot, Gerard Oude Meijers, Dr. Ramon Hofstra, Dr. Cees Beisheuvel, Arco Krijgsman and Otto van Donselaar who have helped me on various occasions on various aspects during the past four years. I have to specially thank Jacob Couperus for helping me on various technical problems involving electronics in my experimental

setup.
I was fortunate to have room-mates with whom I shared good camaraderie, during the past four-year stay in the Netherlands. I was really lucky to have shared apartment with Venkat, Shankar and Vishnu. I would also like to thank my other Indian friends Anand, Ragav, Murali, Amol, Ajay, Jiten, Pramod, Kavitha, Kiran and all the other Indians at the University of Twente.
Most importantly, I am grateful to my family back home in India who were understanding and always encouraged me in all my endeavors. I am indebted to my mother A. Mangalam, brother A.Ashok, sister S. Anandhi, brother-in-law M. Sivakumar and my nieces Lekha and Swetha.

Contents

Chapter 1

Introduction

Real-time, sensitive and selective detection of molecular trace gases in complex gas mixtures at ambient pressure is of importance for numerous fields of application such as breath analysis for medical diagnostics, environmental monitoring and industrial process control. Standard methods such as gas chromatography and mass spectrometry offer a high sensitivity and selectivity, but these two methods are far too slow for real-time measurements. However, real-time detection of trace gases should be possible with laser spectroscopic methods. The reasons for this is that a majority of gas molecules exhibit their strongest fundamental rotational-vibrational bands in the mid-infrared (mid-IR) spectral region of 3 – 5 μm, which is also known as the molecular fingerprint region. This term expresses that gases can be uniquely identified in this region because each specific gas molecule shows a series of distinct, strong and narrow absorption lines characteristic for that type of molecule. However, measuring minute quantities of trace gas molecules, in particular, in complex gas mixtures are challenging because often the spectral lines of different types of molecules can overlap. To still allow a reliable identification of the several gas species it is required that mid-infrared light sources become available which can be rapidly tuned over wide ranges to record absorption spectra of the gas sample that can

uniquely be deconvolved into the components generated by the individual species. For such deconvolution it is important to look at the spectral bandwidth which the mid-IR source should not exceed. At ambient pressures, the spectral lines of gas molecules in the mid-IR region typically have a pressure broadened bandwidth of around 500 MHz and a Doppler broadening of below 100MHz. Thus, for the unambiguous identification of absorption lines the spectral bandwidth of the light source should be less than 100-500MHz depending on the pressure. When looking in more detail, for optically analyzing complex gas mixtures a highly specific light source is required, which simultaneously possess all of the following properties:(1) Watt-level power to ensure a high signal-to-noise ratio for detecting light absorption for with high sensitivity in short (milli-second) time intervals; (2) high spatial coherence, i.e a fundamental Gaussian beam output, for enabling optical signal enhancement techniques such as in multi-pass and resonator enhanced detection; (3) high temporal coherence, i.e., a narrow spectral bandwidth less than 100-500 MHz for unambiguous identification of gases; (4) rapid wavelength tunability with tens of Hz sweeping rates giving access across the entire 3–5 μm region for detection of gases in real-time; (5) the source has to show stable performance over a long time (minutes to hours) and (6) be compact and efficient for being useful in real applications. In summary, when looking at all these requirements to be satisfied simultaneously, it is understandable that such a source does not exist yet and that currently a number of approaches are being explored to reach this goal.

These approaches can principally be divided into two different classes. In the first, coherent mid-IR radiation is generated directly by lasers such as gas lasers, semiconductor lasers, or with rare-earth and transition-metal doped solid-state lasers. In the second approach, coherent mid-IR radiation is generated via optical parametric downconversion of near-infrared (near-IR) laser sources ($\approx$ 0.9 –2 μm).

To name a first example, mid-IR CO gas-lasers have been used for de-

tecting gases in minute quantities [1], but such lasers can only be tuned close to the CO emission lines where the spectral overlap with strong lines from trace gases is usually limited. In contrast radiation provided through semiconductor lasers such as lead-salt, antimonide and quantum-cascade laser show a much improved coverage in the mid-IR and have been used for trace gas measurements. However, common to all these lasers is a relatively low (milli-Watt level) output power and the requirement to operate at cryogenic temperatures [2, 3, 4]. Although recently quantum-cascade lasers have been operated at room-temperatures, spectroscopic detection has been demonstrated only in select regions in the mid-IR [5]. Selective spectroscopic detection has also been demonstrated with rare-earth doped solid-state lasers [6] and mid-IR tuning has been demonstrated with transition metal doped solid-state lasers [7]. But, in all the above lasers, mid-IR tuning is limited to certain gaps in the broad spectral region of interest.

The situation is rather improved when non-linear optics is applied. The reason is that here light amplification can be achieved throughout the entire transparency range of the non-linear crystal which, for example, in the case of lithium niobate extends from 400nm to about 5μm. Mid-IR radiation is generated by parametric down conversion processes either in optical parametric oscillators (OPOs) or with difference frequency generation (DFG). Both DFG and OPO offer the same wide mid-IR coverage and both bear a high potential to become the sources of choice for optical molecular detection [8, 9]. A first advantage of OPOs over DFG is that only a single pump laser is required to generate the entire range of mid-IR wavelengths from 3–5μm. The second advantage is that OPOs provide a much higher conversion efficiency than DFG.

With their high output power and continuous tuning achieved over large wavelength ranges OPOs have shown rapid progress as useful spectroscopic tools [10, 11]. The most prominent examples are singly-resonant OPOs (SRO), which are simpler to tune than other types of OPOs due to the fact that only one of the three involved waves (pump, signal and idler) is

resonant in the cavity. In particular, when the shorter of the two emitted wavelengths (signal wave) is resonant in the cavity, the longer wavelength (idler wave) can be tuned over the entire 3 – 5 μm region. Such a wide tuning can be achieved with various alternative methods, i.e., via changing the crystal temperature, the poling period of the crystal and via the pump wavelength [12, 13]. While the first two methods enable only slow tuning, pump tuning is of utmost importance here because, if the pump wavelength can be tuned fast, this yields a rapid tuning in the mid-IR region as well. More specifically, an SRO exactly copies the line width and tuning properties of the near-IR pump towards the mid-IR output of the OPO, which implies that all of the required mid-IR tuning and bandwidth properties can essentially be achieved by a corresponding control of the OPO pump source in the near-IR. Thus, for an ideal mid-IR generation via an SRO to be used for trace gas measurements, it is required to provide frequency agile near-IR pump sources which meet the named mid-IR requirements regarding linewidth, tuning range and the tuning speed. However, the high Watt-level threshold power of SROs impose the additional requirement that these pump sources also operate at multi-Watt-level power levels to efficiently generate the desired mid-infrared radiation.

Near-IR lasers, such as thin-disk lasers easily provide multi-Watt-level output power and have been used as a pump source for an SRO to perform mid-IR spectroscopy [14]. These thin-disk lasers also offer a narrow spectral line width making them attractive pump sources for high resolution mid-IR spectroscopy. However, it is difficult to achieve rapid wavelength tuning, for instance by electronics means, as compared to lasers based on media that provide extremely high gain, such as in fiber or diode based systems. High power fiber lasers with wide and rapid tuning have been successfully used to pump OPOs and thereby transfer the tuning capabilities to the mid-IR [15]. However, the spectral bandwidth of such fiber lasers and thus also the mid-IR SRO output is too broad to resolve and detect trace gases at ambient pressure. In contrast to this, diode oscil-

lators in the near-IR satisfy most of the requirements such as narrow line width with single longitudinal mode operation,wide tuning range and rapid tunability by all electronic means, along with excellent long-term spectral and power stability. On the other hand diode lasers with such preferable properties are restricted to output powers typically in the milli-Watt range, which is about three orders below the threshold power of an SRO. To solve this problem, the low power of such diode oscillators should thus be amplified in a suitable power amplifier to reach the multi-Watt level. Recent advances in fiber technology have made it possible to realize single-pass amplification to span these three orders of magnitude. Thus, two-stage pump systems consisting of a master-oscillator based on diodes and power-amplifier based on fibers appear rather attractive as a ideal near-IR pump sources for SROs. Following this route, very recently, a narrow line-width DFB fiber- oscillator fiber-amplifier system was used as a pump source for an SRO and over 60 GHz of rapid mode-hop free tuning was demonstrated over the range of 2.65 – 3.2μm [16]. However, the limited pump tuning $< 1nm$ limits mid-IR tuning.

In the present thesis, novel diode-oscillator fiber-amplifier based master-oscillator power-amplifier (MOPA) systems were developed and characterized. This thesis is organized as follows: Chapter 2 starts with a brief discussion on OPOs and SROs with a description of concepts and pump source requirements for enabling rapid tuning of the mid-IR OPO output. This is followed with a short discussion of the different diode based tunable oscillators used so far to control the tuning of SROs, followed by a brief description of improved diode oscillators used in a diode-fiber MOPA setup. The properties of the used fiber amplifier, based on Ytterbium-doped fiber are discussed in detail. Importantly, this includes a discussion of the unwanted non-linear effects prevalent in high-power fiber amplifiers and suggests methods to suppress these non-linear effects. In chapter 3, the Ytterbium doped amplifiers used in all the MOPA setups is characterized and the dependence of the non-linear effects on various parameters

such as the length of the fiber, seed laser power and the seed laser bandwidth is described. Further, the suppression of non-linear effects by spectral broadening achieved through modulation of the seed diode laser is also presented. In chapter 4, detailed investigations into the effect of modulation properties on the DBR diode laser line width are presented. In addition to suppressing non-linear effects, the role of modulation in obtaining broadened spectra with selectable line shapes such as a Gaussian, rather than a U-shape obtained with conventional sinusoidal modulation, is presented. Limitation of the spectral broadening when using large modulation currents is also addressed. Chapter 5 describes the first demonstration of amplification of a broadly tunable actively mode-locked diode laser around 1 μm region. Here picosecond pulses produced from the diode laser are amplified to multi-Watt-levels over most of the tuning range. Chapter 6 introduces a rapidly tunable oscillator based on a broad-bandwidth semiconductor amplifier achieved through an intra-cavity acousto-optic tuning element. In Chapter 7, we discuss the summary and outlook of the various diode-fiber based MOPA systems.

Chapter 2

Review of mid-IR SROs and pump laser systems

This chapter gives an overview on the individual components of a tunable mid-IR light source based on a near-IR diode-oscillator fiber-amplifier MOPA system followed by a singly resonant optical parametric oscillator (SRO). In the first section 2.1, we review the principle and properties of an optical parametric oscillator (OPO). We also discuss the role of an SRO in realizing our goal of wide and rapid mid-IR tuning and, finally, the requirements to be imposed on the near-IR pump laser source. In section 2.2 the different tunable pump oscillators that may be used to pump tune an SRO are briefly described. The choice of a pump source based on diode oscillator in a master-oscillator power-amplifier setup is also presented and the various diode based oscillators developed to pump tune the SRO are presented. In the next section 2.3, the advantage of employing fiber based power amplifier, in particular, Ytterbium-doped fiber amplifiers to amplify the near-IR diode oscillator is discussed. This is followed by a brief discussion of unwanted non-linear effects associated with these amplifiers and the various methods to suppress these non-linear effects in section 2.4.

2.1 Mid-IR generation by an OPO

Our goal of generating widely and rapidly tunable coherent mid-IR radiation is best realized via an OPO as was explained via comparison with other options in chapter 1. The operation of OPOs and its details is extensively discussed in literature [17, 18, 19, 20]. Therefore, here, we recall only the basic working principle and tuning properties of OPOs. This includes a discussion on the various types of OPOs and the specific suitability of singly resonant OPOs (SROs). After the choice of the non-linear crystal, capable of delivering radiation in the desired wavelength range, the requirements for the near-IR pump laser such as the wavelength range and the output power are specified.

2.1.1 Basic principle

An OPO is based on non-linear parametric down-conversion of a strong pump wave in a suitable medium showing a large second order non-linear susceptibility, usually a non-linear crystal. This interaction can be described as a stimulated inelastic scattering of a pump photon $\hbar\omega_p$ by the crystal, where a pump photon of frequency ω_p is absorbed and two new photons with frequencies ω_s and ω_i known as signal and idler photons are generated, respectively. Because of energy conservation the signal and idler frequencies are related to the pump frequency ω_p by

$$\omega_p = \omega_s + \omega_i \tag{2.1}$$

The parametrically generated photons with ω_s and ω_i can build up to macroscopic coherent waves, i.e., a parametric gain is generated at ω_s and ω_i, if the phase matching condition

$$\overrightarrow{k}_p = \overrightarrow{k}_s + \overrightarrow{k}_i \tag{2.2}$$

is fulfilled, which represents conservation of momentum for the three photons involved. For a given wavevector $\overrightarrow{k}_p$ of the pump wave, the phase-matching condition Eq(2.2) selects a narrow band pair of signal and idler

frequencies out of the infinite number of possible combinations $\omega_s + \omega_i$ that are allowed by Eq(2.1). The most efficient parametric generation is achieved, when the three beams are collinear. In this case, the phase matching equation(2.2) can be reduced to its scalar form given by

$$n_p\omega_p = n_s\omega_s + n_i\omega_i \tag{2.3}$$

where n_p, n_s, n_i are the refractive indices of the pump, signal and the idler waves, respectively. Often it is possible to find birefringent crystals with a suitable dispersion where collinear phase-matching Eq(2.3) is fulfilled, if one out of the three linearly polarized waves has an orthogonal polarization and if the waves propagate along a suitable direction with respect to the optical axis of the crystal. This type of phase matching is referred to as birefringent phase-matching (BPM) [17].

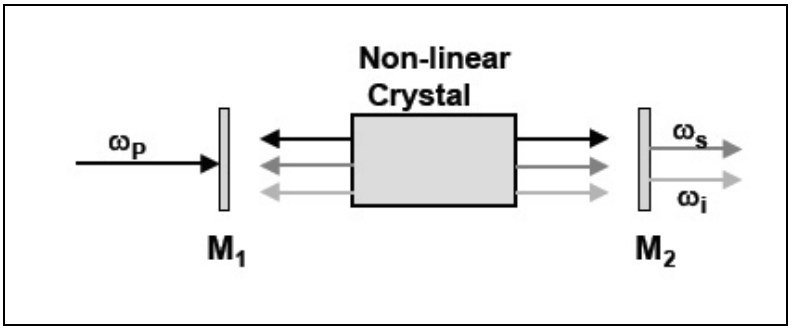

Figure 2.1: Schematic diagram of an OPO, ω_p is the pump wave generating the signal wave ω_s and the idler wave ω_i. M_1 and M_2 are the cavity mirrors.

To form an OPO, the non-linear crystal is placed inside a resonator as shown in Fig 2.1. Parametric oscillation on the signal and idler frequencies can start when the parametric gain for the signal and idler waves exceeds the total cavity losses. The pump power required to start this oscillation is known as the threshold power of the OPO. The threshold power is strongly dependent on number of the waves resonant in the cavity. The optical cav-

ity can be resonant either for one wave (singly resonant OPO, SRO), two waves(doubly resonant OPO, DRO) or for all the three waves (triply resonant OPO, TRO). The threshold power becomes lower with an increasing number of resonant waves in the cavity. To give some typical examples, the threshold power for a continuous-wave SRO is around 3W [21], for a DRO it is up to 100 times lower, but typically around 100mW [22] and it is around 1mW for TROs [23]. On the first impression this seems to indicate that the operation of an SRO, instead a DRO or TRO, would be a disadvantage, due to the much higher pump power required. However, SROs offer the important advantage of a superior spectral and power stability [24]. In comparison, DROs in which the signal and the idler waves are resonated have much lower amplitude and spectral stability, which is due to the effect of spectral clustering [25, 26]. For the same reason DROs pose severe difficulties with regards to their tuning behavior. In summary DROs can be ruled out as a convenient spectroscopic sources because they require highly stable pump powers, carefully engineered cavities and multiple control loops for good spectral and power stability [27]. Furthermore, even in these advanced setups, the complexities increase when continuous (mode-hop free) tuning over ranges larger than typically 10GHz is to be achieved [28]. TROs suffer from the same problems faced in DROs, while the additional resonant wave makes tuning all the more difficult.
In contrast, wide continuous wavelength tuning in SROs is easily accomplished together with high power and spectral stability [29], once one is capable to provide high quality, widely tunable and powerful pump radiation. In view of these arguments, for our goal of frequency agile generation of mid-IR wavelengths, we consider only SROs with their cavity resonant for the signal wave, while the pump and idler waves perform a single pass through the crystal. As a consequence, this thesis deals with the central challenge to provide, powerful and rapidly tunable pump radiation via various approaches involving diode laser oscillators and fiber amplifiers.

2.1.2 Phase-matching

To discuss the possibility for wavelength tuning of OPOs, we briefly recall how the spectral gain of an OPO can be tuned. The gain of the signal and the idler waves depends on the pump intensity and on the effective non-linear susceptibility of the crystal, when perfectly phase matched (i.e. $\Delta\overrightarrow{k} = \overrightarrow{k}_p - \overrightarrow{k}_s - \overrightarrow{k}_i = 0$). For non-zero phase match (i.e. $\Delta\overrightarrow{k} \neq 0$ but small), the signal and idler waves experience a lower parametric gain as compared to perfect phase matching. The decrease in gain due to the phase-mismatch $\Delta\overrightarrow{k}$ is approximately (parametric interaction of plane, non-focussed waves in a crystal with spatially constant non-linearity) given by

$$gain \propto sinc^2(\left|\Delta\overrightarrow{k}\right| L_C), \tag{2.4}$$

where L_C is the length of the crystal. As a result of Eq(2.4), the threshold for an SRO with non-zero $\Delta\overrightarrow{k}$ is higher as compared to the perfectly phase-matched case. Therefore, when no further frequency selective elements are present, an SRO oscillates at those signal and idler frequencies where $\Delta\overrightarrow{k}$ is minimum. Thus, an SRO can be tuned by changing the refractive indices of the three waves as seen in Eq(2.3). This can be accomplished, for example, by changing the temperature of the crystal or the directions of beams propagating in the crystal via a rotation of crystal in the cavity. During such tuning, the resonant wave performs mode-hops and the other wave performs corresponding frequency hops if no further measures are taken.
The initial fundamental developments in the field of OPOs were performed using birefringently phase matched crystals such as MgO:LiNbO_3, LBO, and KTP by which a good spectral coverage of the mid-IR spectral range is possible. More recently, the development of quasi-phase matching (QPM) materials such as periodically poled LiNbO_3(PPLN), PPKTP and PP$LiTaO_3$ led to a substantial widening of the spectral coverage [30, 31]. QPM is a technique in which the phase mismatch between the waves is corrected at regular intervals using a structured spatial periodicity (poling period) built into the non-linear medium along the propagation direction of the beam.

By choosing a suitable value for the poling period Λ (also known as grating period) according to

$$\Lambda = \frac{2\pi}{\Delta k}, \tag{2.5}$$

periodic phase changes of the non-linearly induced polarization ensure that the signal and idler waves generated are on average in-phase throughout the entire propagation length in the crystal. Such crystals typically consists of periodic domains with opposite orientation of the crystal axis, and are fabricated by the so-called field poling technique. This technique allows to pole the crystal with any desired domain structure such as a periodic poling with a spatial period Λ. As a result, for a QPM crystal, the BPM condition Eq(2.3) is replaced by a much more general, effective phase-matching condition given as

$$\Delta k' = 2\pi(n_p\omega_p - n_s\omega_s - n_i\omega_i - 1/\Lambda) \tag{2.6}$$

From this expression it can be seen that QPM has several important advantages over BPM. Within the entire transparency range of the crystal material, QPM can be achieved for any desired signal and idler wavelength pair fulfilling energy conservation Eq(2.1), and is no longer limited by the natural birefringence and dispersion of the non-linear crystal used. As a consequence all the three waves can have the same polarizations. This gives access to the highest coefficient of the $\chi^{(2)}$ non-linear tensor while BPM is restricted to coefficients of much lower value. This results in high parametric gain, and in an OPO, results in a reduced pump threshold with high conversion efficiency and output power. Hence, we use QPM crystals for our OPOs. For convenience and its commercial availability as long crystals, we consider here periodically poled lithium niobate (PPLN). This material has been successfully used to operate SROs with a threshold of a few Watts in the 3-5μm mid-IR region of interest here, using pump sources around 1.064μm [32]. The various tuning methods that enable to access the mid-IR over the given 3-5μm range are compared in the next subsection.

2.1.3 Wavelength coverage in PPLN

The wavelength coverage possible with PPLN can be calculated from the phase matching and energy conservation conditions based on the Sellmeier equations (crystal dispersion curves) as described in [33]. The tuning can be achieved by varying the different parameters shown in Eq (2.6) such as the grating period, the temperature dependent dispersion of the crystal and the pump frequency. Fig 2.2 shows an example of the calculated phase-matched signal and idler wavelengths of a PPLN OPO as a function of the grating period while the crystal temperature is held fixed at 450 ^{o}K and the pump wavelength is fixed at 1.08μm.

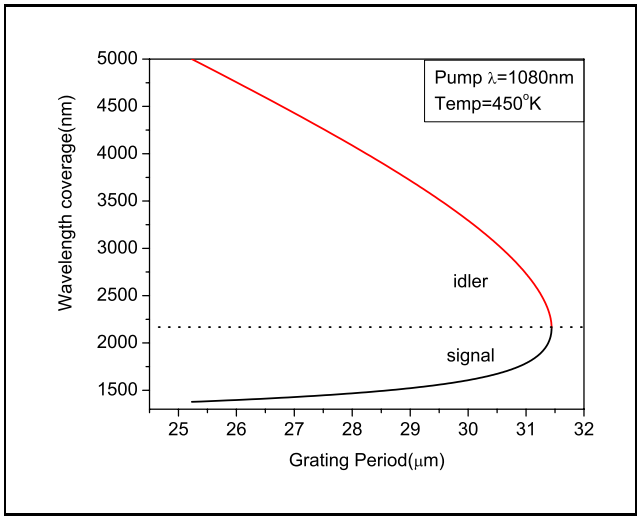

Figure 2.2: The calculated wavelength coverage possible in PPLN via phase matching by varying the grating period of the crystal at a constant value of pump wavelength $\approx 1.08\mu$m and crystal temperature $\approx 450K$

It can be seen that the signal wavelength tunes below the dashed line (representing wavelength degeneracy) and the idler tunes in the mid-IR range (above the line). It can further be seen that the idler wavelength can indeed be tuned over the entire 3-5μm by just tuning the grating period in

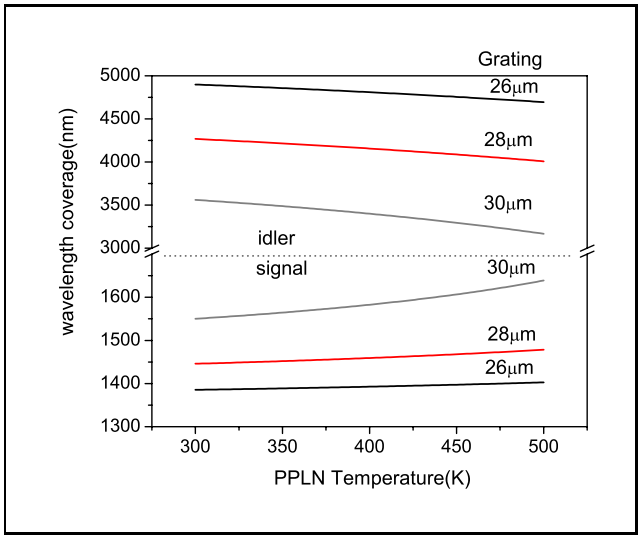

Figure 2.3: The calculated phase-matched signal and idler wavelength coverage possible in PPLN with combined grating period and temperature variation of the crystal at a constant value of pump wavelength $\approx 1.08\mu$m

a range from 25 to 32 μm. As the second tuning alternative, Fig 2.3 shows the phase-matched signal and idler wavelengths vs. the crystal temperature while the poling period and the pump wavelength are held constant. As the temperature varies from 300K to 500K, the idler wavelength tunes over hundreds of nanometers for a single grating period. Although the temperature and grating period tuning methods offer wide wavelength coverage, both tuning methods are rather slow and the grating based tuning often requires a realignment of the OPO. Hence these methods are unsuitable for rapid tuning, where one desires hundreds of nanometers mid-IR tuning in milli-second time intervals.

A sufficiently fast tuning method turns out to be the method of tuning the pump wavelength. Fig 2.4 shows the wavelength coverage achieved by tuning the pump wavelength over tens of nanometers in the near-IR region for a fixed crystal temperature and grating period. It can be seen that this

results in a wide idler tuning over hundreds of nanometers in the mid-IR. Furthermore, an interesting tuning property can be seen, which is the result of the particular combination of the chosen material dispersion (choice of lithium niobate) and the choice of a particular signal wavelength(around 1.6μm) via the poling period. In this case, the tuning of the pump wavelength is almost fully transferred to a tuning of the idler, while the signal wave does not tune much at all. As a result, if the pump wavelength can be tuned fast, the mid-IR idler also tunes at the same fast rate. Hence a rapid tuning in the mid-IR region is possible.

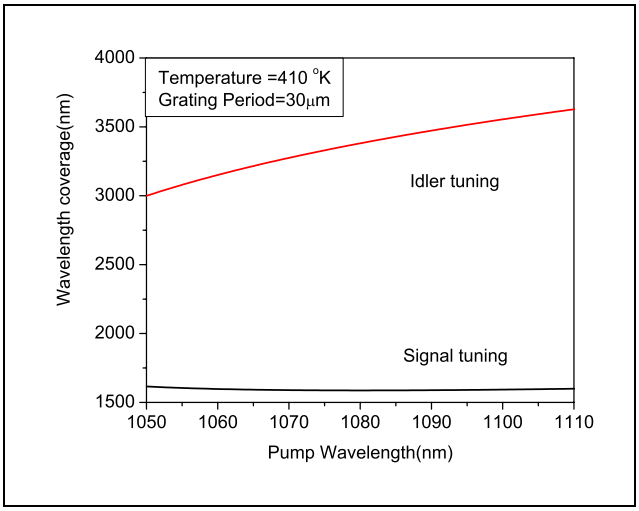

Figure 2.4: The calculated wavelength coverage possible in PPLN with the pump wavelength at a fixed crystal temperature $\approx 410K$ and grating period of 30μm

2.1.4 Tuning in an SRO

In the case of an SRO, the OPO cavity is resonant only for one frequency, which we select to be the signal wave in our considerations by using appropriate mirror coatings. In this case the signal oscillation occurs at the cavity frequency closest to the gain maximum, at the longitudinal modes of

the OPO cavity. For a given pump wavelength, this corresponds to a idler wavelength governed by Eq(2.1) in the mid-IR. By varying the temperature and grating of PPLN, a coarse wavelength tuning is still possible across the 3-5 μm region as shown in Fig 2.2 and Fig 2.3. PPLN exhibits parametric gain with broad spectral widths of hundreds of GHz. In contrast, the cavity mode spacing (free spectral range, FSR) is of the order of one GHz and oscillation is possible only on one of these equally spaced cavity modes. Varying the various parameters such as the crystal temperature, cavity length and pump frequency can tune the SRO, also an intra-cavity etalon can be used for frequency selection as illustrated schematically in Fig 2.5.

Changing the crystal temperature leads to a change of the refractive indices of the three interacting waves, the pump, signal and the idler waves. This shifts the parametric gain along the frequency axis shown in Fig 2.5. However, by varying the temperature, the signal wave initially remains oscillating in the same cavity mode while the gain maximum moves towards the adjacent cavity mode. This, eventually causes the oscillating signal frequency to hop by one FSR of the cavity and subsequent hops occur with further temperature change. As the pump frequency is held constant, this causes the idler frequency to hop in the opposite direction in steps of the FSR of the cavity. This step-wise tuning is also known as coarse tuning and has been used to obtain tuning over hundreds of nanometers [13].

A finer tuning of the SRO output can be achieved by tuning the cavity length, for instance, with a piezo-control, while the center frequency of the parametric gain remains fixed. This way the SRO can be tuned without a mode-hop up to a maximum frequency change of one FSR. Thereafter, a mode hop occurs and brings the SRO frequencies back to the center frequency of the gain curve.

The third method is by pump tuning, where changing the pump frequency shifts the parametric gain maximum along the frequency axis. As with temperature tuning, the signal remains oscillating in the same cav-

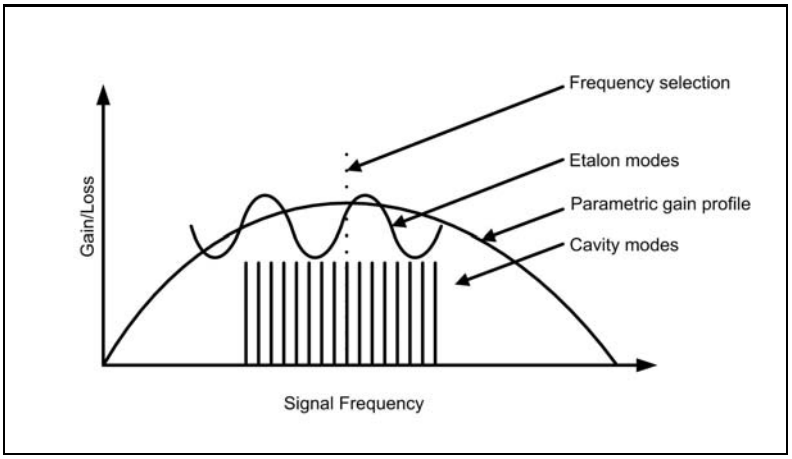

Figure 2.5: Frequency selection in an SRO.

ity mode (closest to gain maximum) until the gain has shifted by more than one FSR. However, different from temperature tuning, the idler frequency tunes continuously along with the pump frequency, until the signal encounters a mode-hop. Here there are two ways to obtain a wide range of continuous idler tuning. In the first, an intra-cavity etalon is introduced in the OPO cavity with $FSR_{etalon} >> FSR_{cavity}$ as shown in Fig 2.5. The etalon introduces frequency selective losses in the cavity. As a result, the SRO oscillates with its signal wave in a particular cavity mode near to the gain maximum, while the etalon loss introduced at the other cavity modes over wide range (the FSR of the etalon) ensures that no other signal mode can start to oscillate, although the pump wavelength tunes the gain maximum. Hence a large mid-IR idler tuning is achieved without mode-hops when a continuous tuning of the pump is assumed. A large mid-IR continuous tuning over 60 GHz has been obtained this way [16]. In addition, when the pump laser is tuned fast, while the signal frequency is fixed via the etalon, the idler tunes at the same fast rate. Indeed, the 60GHz continuous tuning mentioned, was available as rapid tuning. In this case, the pump laser was swept over the 60 GHz interval 30 times per second, such that 30

idler absorption spectra per second could be recorded with a suitable line absorbing molecular gas.

In the second method, by appropriate choice of the signal frequency, the gain maximum tunes much slower than the pump frequency (see Fig. 2.4). The signal remains oscillating at the same cavity mode for a broader pump tuning range. In this situation, even when the signal frequency hops over one FSR the idler tunes much more than one cavity FSR. Based on this, a wide and rapid continuous tuning over 110 GHz in the mid-IR was obtained, which is the current record for mode-hop free mid-IR tuning with continuous-wave OPOs [34].

It can be seen that, for PPLN according to Fig 2.4, for a fixed crystal temperature when the pump is tuned over tens of nanometers, the idler tunes over hundreds of nanometers, while the variation in the signal is only a few nanometers. With PPLN the signal change is minimal with pump wavelength around 1080nm which is, incidentally, also the wavelength of maximum available fiber gain, when using an Ytterbium-doped fiber amplifier.

These considerations clearly show what properties a pump source has to possess, when a wide, rapid and mode-hop free tuning of the idler wave from a PPLN based SRO is to be achieved, to be useful in spectroscopic applications. These SROs require a pump source that 1) operates at wavelength around 1.08μm, which 2) provides the capability of large continuous near-IR tuning and which offers 3) a multi-Watt-level output power to surpass the threshold pump power of the SRO. Further, 4) a rapid tuning of the pump source is desired. This is difficult to achieve with opto-mechanical approaches, such as piezo-controlled gratings, but it might be obtainable with electronic tuning methods.

In the next section, various pump sources used for SROs and the considerations that led to our particular choice of the pump laser source, a diode-oscillator fiber-amplifier system, are discussed. The spectral and tuning characteristics of the pump source are provided by the diode oscillator,

while the fiber amplifier provides the multi-Watt output power needed to overcome the SRO threshold power.

2.2 Tunable pump laser sources for operation of SROs

In the previous section it was explained that operating an SRO with a wavelength tunable pump laser is rather attractive and successful to arrive at wide and rapid tuning in the mid-IR region of 3-5μm. This identifies the development of suitable pump sources tunable in the near-IR, as being of central importance for mid-IR spectroscopic applications.
Therefore let us summarize more precisely the specifications that a suitable pump source needs to possess. First, the pump laser should have a sufficiently high power of 3 to 5W which is the typical threshold power of an SRO based on PPLN and emitting in the mid-IR. Second and third, the pump laser should operate and be tunable over tens of nanometers in a wavelength range around 1.08μm. In addition, for being applicable for real-time spectroscopic identification of trace gases at atmospheric pressures, the mid-IR radiation must satisfy two additional requirements which is a sufficiently narrow line-width between 100 and 500MHz, enough to resolve the molecular absorption lines at atmospheric pressure, and a rapid tunability with hundreds of nanometers in milli-second intervals. Both can be realized when the SRO pump source shows these properties i.e., narrow linewidth and high wavelength agility. The latter is best to be achieved with electronic means. In contrast, mechanical tuning methods often are limited in speed due to inertia of masses of the opto-mechanical components such as piezo-driven mirrors and gratings. Also, a tuning by electronic means is often more reliable compared to mechanical means, because mechanical tuning can lead to frequency jitter, due to vibrations involved, when tuning rates of the order of tens of nanometers in milli-second time intervals (ms rates) are to be achieved. The pump laser requirements are summarized in

the Fig 2.6.

In order to motivate our particular choice for specific types of pump

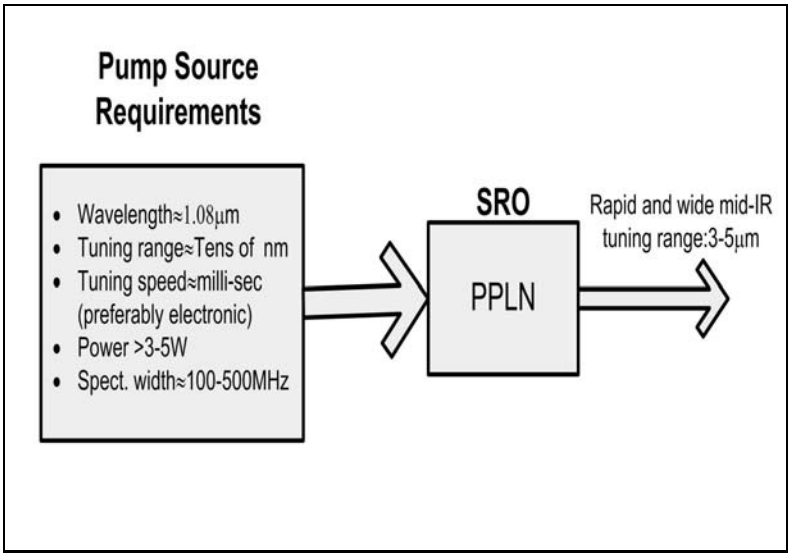

Figure 2.6: The requirements of the SRO pump source for application in real-time trace gas detection

laser systems, let us review what other types of pump lasers have been used so far for operating SROs. Thin disk lasers provide a broad tuning range of more than ten nanometers, with narrow spectral width (5MHz), and high output powers (20 W) have been used to pump-tune SROs for mid-IR spectroscopy [14]. However, it remained difficult to achieve rapid wavelength selection, because rapidly tunable wavelength filters often produce high round-trip losses, which would significantly reduce the output from such thin disk lasers due to their relatively low-gain per round-trip. High intra-cavity losses are much easier to tolerate in laser oscillators with high round-trip gain, such as fiber or diode based oscillators. To give an example, fiber oscillators with wide and rapid tuning via an intra-cavity acousto-optic tunable filter (AOTF) had been used to pump tune an SRO, by which wide and rapid tuning in the mid-IR was achieved [15]. However

the frequency selectivity of these AOTFs is rather low, rendering a larger pump bandwidth, and thus also a larger spectral width (>30 GHz) of the generated mid-IR radiation. This is usually too large to resolve and detect trace gases at ambient pressures, but it may be sufficient to analyze the trace gas content of certain industrial gas sample at high (tens of bars) pressures. More recently, a distributed feedback (DFB) fiber oscillator with narrow spectral width and 60 GHz continuous tuning range followed by a fiber amplifier had been used to pump tune an SRO and a rapid and continuous tuning of around 60 GHz in the mid-IR had been reported [16]. In comparison, some diode based laser oscillators satisfy most of the spectral requirements such as narrow spectral width, wide and rapid (all electronic) tuning, along with good temporal and spectral stability. However, they offer only low output power in milli-Watt range which is three orders of magnitude below the typical threshold of an SRO. The most obvious way to overcome this problem is to amplify the oscillator output in a diode amplifier. This approach proved successful to some extent, as can be seen in Ref [35]. However, diode amplifiers are limited so far to power levels of a few Watts only and deliver output beams of reduced spatial quality. Correspondingly, the SRO described in Ref [35] was designed for providing a low threshold (≈500 mW), and for this purpose the idler output had to be set to a spectral range (≈ 1.9μm) of less importance for trace gas detection. As a potential solution to this limitation of high power diode amplifiers, significant progress in the field of fiber amplifiers has made it possible to obtain single-pass gain of over three orders of magnitude. Thus, it seems highly attractive to envision diode laser oscillators followed by high power fiber amplifier as master-oscillator power-amplifier (MOPA) systems, to pump tune SROs for real-time spectroscopy.

In the next subsection, we briefly dwell on the various different types of tunable diode oscillators that come into consideration for such diode-fiber MOPA systems and discuss their their suitability to enable real-time detection of trace gases across the 3-5 μm range. In section 2.3, the advantage

of employing fiber technology, in particular double-clad Ytterbium doped fiber amplifiers, is discussed. The next section 2.4 includes a brief discussion of unwanted non-linear effects that can easily occur with these fiber amplifiers and we present ways to suppress these non-linear effects.

2.2.1 Pumping SROs by tunable diode lasers

Diode based tunable oscillators are preferred in a MOPA system to pump OPOs for following reasons. With constant operation parameters they offer stable wavelength operation, but they can also be tuned over a wide wavelength range, achieved by varying either the pump current or the diode temperature, such as in solitary Fabry-Perot (FP) diode lasers [36]. The tuning capabilities of FP diode lasers can be enhanced greatly, and the spectral linewidth can be narrowed, by incorporating a grating (external or internal to the laser chip) [13, 34]. When the grating is placed external to the diode the device is called an external cavity diode laser (ECDL). When the grating is incorporated in the chip the laser is called a distributed Bragg reflector (DBR) diode laser or a distributed feedback diode laser (DFB) [37, 38]. In an ECDL, the output facet of the diode laser is antireflection-coated to eliminate optical feedback, while the grating acts as a narrow wavelength selector which determines the specific operating wavelength out of the usually broad gain spectrum of the semiconductor material [39]. Such an ECDL followed by a semiconductor tapered amplifier has been successfully used to pump-tune an SRO, mode-hop free, over 56 GHz [13]. Here, the tuning of the laser had been accomplished by mechanical means, ie., by a piezo-controlled tilt of the grating. However this can lead to frequency jitter induced by mechanical resonances in the setup. Moreover, such an ECDL does not lend itself to be rapidly tuned, due to the limited speed of piezo-driven mechanics. Finally, the output power of current tapered diode amplifiers is limited to only a few Watts which is only slightly above the threshold pump power of SROs and thus leads to a relatively small conversion efficiency from the near-IR pump to

the to the mid-IR idler output power generated from the SRO.
In view of these disadvantages we started to investigate DBR diode lasers with fiber amplification. DBR diode lasers possess the advantage that they are monolithically integrated devices and thus are largely insensitive to external mechanical perturbations. Further, the built-in grating section and phase section can be tuned all-electronically which offers, unlike with an external grating, a fast wavelength tuning and little wavelength jitter. Indeed, in our previous work, a fiber-amplified DBR diode laser driving by SRO was successfully used to obtain a mode-hop free tuning in the mid-IR over a range of 110 GHz, scanned across within 29 ms [34]. Although this is still the widest mode-hop free tuning range ever achieved with an OPO, the coarse tuning range of the DBR diode laser was limited to only 2nm around 1080 nm by the internal grating. This limited the mid-IR tuning range of the SRO. To cover wider wavelength ranges in the mid-IR, the pump laser should tune at least over tens of nanometers while still providing rapid tuning. This led to our investigation of widely tunable diode-based near-IR oscillators with external feedback, where high speed intra-cavity frequency selecting elements access the desired wavelength range within the broadband (tens of nanometers) gain spectrum of the diode.
In particular, we present a rapidly tunable near-IR diode oscillator based on a broad-band semiconductor tapered amplifier. A quickly tunable acousto-optic tunable filter (AOTF) acts as an intra-cavity frequency selective element. The semiconductor amplifier is placed in an unidirectional cavity, that includes the AOTF and an solid-state etalon. This enables to obtain wide tuning over almost the entire gain bandwidth of the semiconductor amplifier with narrow spectral width and high tuning rates. A detailed characterization of the near-IR oscillator is presented in Chapter 6. The tens of mW output power of these diode lasers is amplified in a double-clad Ytterbium-doped fiber amplifier to multi-Watt levels. In addition to amplifying this diode oscillator, we experimentally investigate the fiber amplification of two alternate diode oscillators. The first is a DBR diode laser,

which was used to characterize the amplifier in chapter 3. In chapter 4, we describe how this DBR diode laser is used to generate controlled spectral shapes such as Gaussian or U shapes, through current modulation with specific modulation waveforms. The second oscillator is an AR-coated FP diode (ECDL), which is mode-locked by fast (GHz) current modulation to produce picosecond pulses tunable around the 1μm region (see chapter 5).

2.3 Ytterbium doped fiber amplifier

This section on Ytterbium doped fiber amplifiers is divided into 3 subsections. In the first, the basics of fiber amplifiers are discussed. In the second, the advantage of Ytterbium doped fiber amplifiers over other fiber amplifiers or bulk amplifiers are discussed. This is followed by a discussion of the various unwanted non-linear effects that can occur in these fiber amplifiers and the methods for their suppression.

2.3.1 Basic properties of fibers and fiber amplifiers

An optical fiber consists of a central glass core surrounded by a cladding layer whose refractive index n_2 is slightly lower than the core index n_1. Such fibers are generally referred to as step-index fibers. Fig 2.7 shows schematically the cross-section and refractive index profile of such a fiber. A detailed discussion of light propagation in optical fibers can be found in Ref [40].

Two parameters that characterize a step-index fiber are the numerical aperture (NA) defiened as

$$NA = \sqrt{n_1^2 - n_2^2} \tag{2.7}$$

and the V-parameter defined as

$$V = k_0 a \sqrt{n_1^2 - n_2^2} \tag{2.8}$$

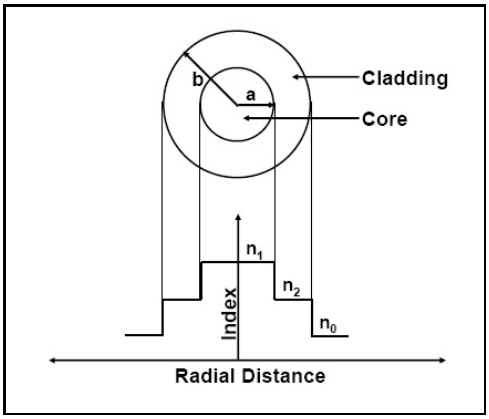

Figure 2.7: Schematic illustration of the cross section of an refractive index profile of step index fiber.

where $k_0 = 2\pi/\lambda$, a is the core radius and λ is the wavelength of light. The numerical aperture determines the maximum acceptance angle of the fiber for the light to propagate in the fiber. The V-parameter determines the number of modes supported by the fiber. A step-index fiber supports only a single mode, if $V < 2.405$. Optical fibers designed to satisfy this condition are called single-mode fibers. Eq(2.8) shows that at a given wavelength the main difference between a single-mode and multimode fibers is the core size. For wavelengths, around 1μm, the core radius a is typically 25-30 μm in multimode fibers, whereas single-mode fibers require $a < 5\mu$m. Light is guided in the core by the principle of total-internal reflection, along the entire length of fiber, which can range anywhere between several centimeters to kilometers. Light from a input laser oscillator, also called signal (not to be confused with the signal wave of an OPO), can be amplified in the fiber, by incorporating laser active ions in the fiber core and creating a population inversion via optical pumping of the ions with another light wave (pump wave) that is guided through the fiber as well. The rate of stimulated emission in any light amplifier scales proportional with the pump and signal wave intensities, i.e., the greater these intensities, the higher the

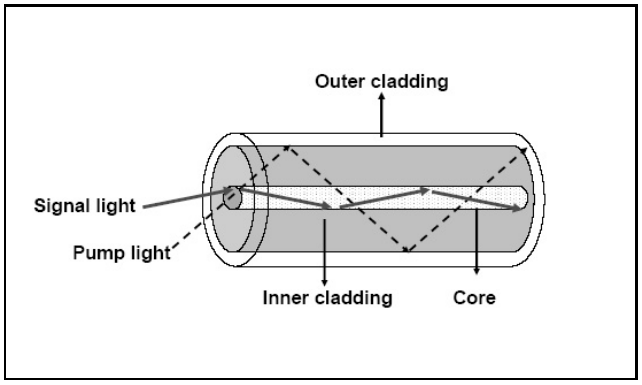

Figure 2.8: Schematic illustration of amplification in a double clad fiber. The signal light which is coupled into the fiber core is amplified by the pump light, which is coupled into the inner-cladding and absorbed by the doped core of fiber.

probability of interaction between an inverted ion and a signal photon, and the higher the optical gain. In a bulk amplifier, i.e., a conventional laser crystal, the interaction length between signal and pump intensities is limited by the diffraction of the beam. In comparison, in an optical fiber, the signal and the pump light is confined by waveguiding in the fiber core over the entire length of the fiber. This property leads to high gain per unit-length and thereby makes it possible to realize lasers with low threshold and high gain amplifiers with low pump power requirements. The other significant advantages include a compact size of fiber setups and the potential for excellent mechanical and thermal stability due to the properties of the glass host.

The amplification in an optical fiber whose core is doped with active ions is determined by the amount of pump power that can be effectively coupled into the core and there overlaps with the signal. However, it turns out that a single-mode fiber of the type shown in Fig(2.7) is of little use in connection with high power multimode pump sources, due to low efficiency of coupling

multimode pump light in to the single mode fiber core. This problem led to the development of the so-called double clad fiber technology, which has tremendously increased the output power available from fiber lasers and fiber amplifiers [41, 42]. The different design of a double clad optical fiber is depicted in Fig(2.8). Again there is a core which is doped by laser active ions, there is a cladding layer surrounding the core, the so-called inner-cladding, but there is an additional outer-cladding layer surrounding the inner cladding layer such that the outer-cladding has a lower index than the inner cladding. A relatively large diameter along with a high NA of the inner-cladding supports many fiber modes in that inner-cladding. Hence, light from high power pump diodes that typically has only a low beam quality can be efficiently coupled into the inner-cladding of the fiber. The pump energy confined inside the inner cladding also traverses the core as shown in Fig 2.8, such that dopant ions in the core are pumped. This way of pumping the inner core is usually called cladding pumping. The signal propagates only in the fiber core, where it becomes amplified. Cladding pumping can be utilized in fiber amplifiers, and such amplifiers can be employed to build high-power single spatial mode fiber lasers.

In the described double-clad fibers, the absorption of pump light by the core is dependent on the effective overlap between the pump light and the doped core. Pump light propagates in the inner-cladding in basically two ways. In the first, known as meridional rays, the light rays cross the fiber core whose active ions absorb them during propagation along the fiber. The second form of pump propagation is via the so-called skew rays, where pump light rays propagate around the core without crossing it and are thus not absorbed by the core. This reduction in pump absorption, causing a relatively long pump absorption length, can be reduced by inducing a mode-mixing between the meridional and skew rays. This is accomplished, e.g., by using fibers with non-circular inner-cladding such as with a D-shaped cross section [43]. The core dopants are usually optically active rare-earth ions such as Erbium, Ytterbium, Neodymium or Thulium [44].

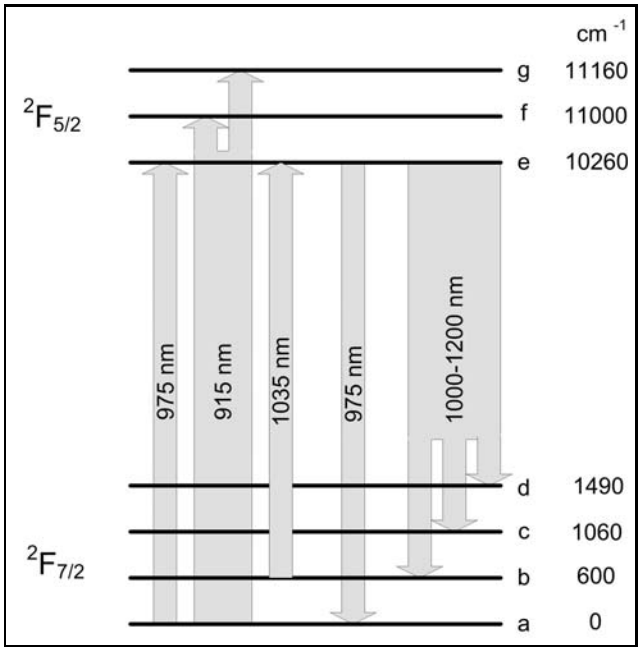

Figure 2.9: The Yb^{3+} energy level structure consisting of 2 manifolds, the ground manifold $^2F_{7/2}$ with 4 stark levels (labeled (a)-(d)) and the excited state manifold labeled $^2F_{5/2}$ with 3 stark levels(labeled (e)-(g)). The approximate energy in wave numbers are indicated above the ground state.

The desired emission wavelength range determines the choice of the doping ions in the fiber core. For amplifying near-IR light in 1–1.1 μm region, Ytterbium doped fiber is preferred, whose properties are discussed in the next subsection.

2.3.2 Properties of Ytterbium doped fiber amplifiers

Ytterbium-doped fiber amplifiers (YDFAs) possess large absorption and emission bandwidths extending from roughly 800 to 1064nm for absorption and from 970nm to 1200nm for emission. Due to the simple energy

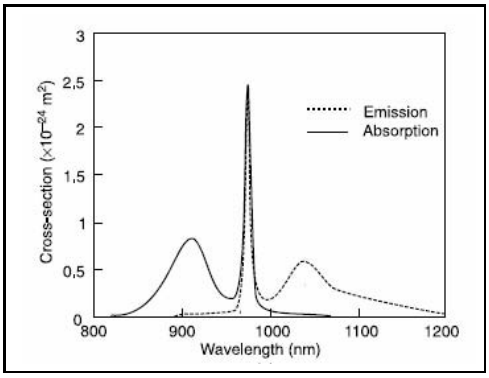

Figure 2.10: Absorption (solid-line) and emission (dashed-line) crossection of Yb^{3+} [45]

level structure of Ytterbium (Yb^{3+}) [46, 45], YDFAs do not suffer much from unwanted competing processes such as excited-state absorption, non-radiative decay and concentration quenching as found in fibers doped with other ions such as erbium-doped fibers. Therefore, Yb-doped fibers can offer comparatively high output powers and high pump conversion efficiencies. The broad gain bandwidth is ideal for amplification of widely tunable near-IR oscillators and ultra-short pulses around the 1-1.1μm region. For a closer discussion of the spectral properties of these fibers, Fig 2.9 shows the relevant energy level structure of Yb^{3+}. It can be seen that, the levels are grouped in two manifolds. The ground-state manifold $^2F_{7/2}$ consists of four Stark levels labeled $(a)-(d)$ in the figure and the well separated excited state manifold $^2F_{5/2}$ consists of three Stark levels labeled $(e)-(g)$. This simple two-manifold system of the Ytterbium ion is what excludes excited state absorption of the pump or signal wavelengths. In addition, the large energy gap of $\sim 10000cm^{-1}$ precludes non-radiative decay and concentration quenching. As a result, the lifetime of the excited $^2F_{5/2}$ level is relatively long, typically around 0.8ms.
In Fig 2.10, the dependence of the absorption and emission cross-section of Yb^{3+} in glass are shown vs. wavelength. It can be seen that the strong

and narrow peak at 975 nm in both emission and absorption corresponds to transitions between the lowest Stark levels (a to e). The strong absorption at this wavelength can be exploited by an efficient pumping of short double-clad fibers with high power diodes. The additional benefit of this choice of pump wavelength is the low quantum defect between the pump and the signal wavelength, which increases the power conversion efficiency and reduces the thermal load in the fiber. The absorption peak at shorter wavelengths, at 915 nm seen in Fig 2.10, corresponds to transitions from level a to f and g in Fig 2.9, while the long wavelength shoulder in the absorption spectrum of Fig 2.10 corresponds to transitions from level b at wavelengths around 1030nm. The weak absorption here is a consequence of a much smaller population at this level: the thermally excited population of level b is only 6 % of that of level a at room temperature according to the Boltzmann distribution. Nevertheless, the thermally excited population plays a significant role in the signal re-absorption loss when inversion is low at weak pumping. This re-absorption reduces the gain and additionally shifts the gain maximum to longer wavelengths at weaker pumping powers.

At a pump wavelength of 975nm, the laser action is truly three-level in character, because light amplification brings population into the lowest stark level. The second peak in emission spectrum, with its tail extending to 1200 nm, corresponds to transitions from level e to b, c and d as shown in Fig 2.9. At longer wavelengths the laser action on these transitions becomes nearly four-level in character, because light amplification brings populations into the levels c and d. The relatively smooth gain spectrum of the Yb-doped silica fibers is attributable to phonon-induced broadening of the individual sub-levels and due to local variations in the Stark splitting. The resulting gain is mainly homogeneously broadened, although some degree of inhomogeneous broadening remains present [45, 47].

Double-clad Yb-doped fiber amplifiers (YDFA) pumped with high power diodes at the peak absorption 975 nm are widely used to obtain high out-

put powers across the 1-1.1 μm wavelength region. YDFAs have been successfully used to amplify continous-wave (CW) and single-frequency signal input beams to over 100 Watts of output power [48, 49]. Even powers of up to the kW levels have been demonstrated in such fibers, although only possible with a broad band signal beam input of elevated power [50]. Of particular importance of the present work is that these double-clad YDFAs are suitable for amplifying the milli-Watt near-IR diode oscillators operating around 1-1.1μm to a multi-Watt output. Such amplification is achieved with high efficiency, typically, with fiber length varying from several meters to several tens of meters as given by the relatively long pump light absorption length in cladding pumped fibers. These long absorption lengths, actually, form a severe problem because the resulting long interaction lengths of the signal wave in the core can give rise to unwanted non-linear effects such as stimulated Brillouin scattering which leads to an uncontrolled output in the form of pulses. Such pulsing is highly undesired, as a stable output power is paramount for spectroscopic applications. In view of the importance to provide a temporally stable output, in the next subsection, we discuss the origin and properties of such non-linear effects in fiber amplifiers and discuss means to suppress them.

2.4 Non-linear effects in fiber amplifiers

Non-linear effects are apparent in cladding pumped fibers due to two experimental parameters: the small core size and the long fiber length. The small size of the fiber core concentrates the signal light into a small area and thus results in rather high intensities. These high intensities are maintained over tens of meters of fiber length, required in cladding pumping to substantial powers, which provides a long interaction length for non-linear effects. These non-linear effects can significantly affect a signal during propagation in silica fiber. The optical response of a medium to intense electromagnetic

fields can be expressed by expanding the light-induced polarization of the medium, in powers of the incident electric field E [51].

$$P = \epsilon_o \left\{ \chi^{(1)} E + \chi^{(2)} EE + \chi^{(3)} EEE + ... \right\} \tag{2.9}$$

where ϵ_o is the vacuum permittivity; $\chi^{(1)}$ is the linear susceptibility and where $\chi^{(n)}$ is the n^{th} order susceptibility. As silica shows an inversion symmetry, even-order susceptibilities such as $\chi^{(2)}$ are absent, and the dominant non-linear effects are governed by the third-order susceptibility $\chi^{(3)}$. The non-linear effects occurring via $\chi^{(3)}$ are usually classified into two different types.

1. Non-linearities arising due to optically induced changes in refractive index, which results either in phase modulation [self-phase modulation (SPM) and cross-phase modulation (XPM)] or in the mixing of several waves and thereby generate new frequencies, such as in four-wave mixing (FWM). [52, 53, 54]

2. Non-linearities arising from inelastic scattering of light by the medium which involves energy exchange between medium and the signal, such as stimulated Raman scattering (SRS) and stimulated Brillouin scattering (SBS) [55].

As with the linear susceptibility, the real part of the $\chi^{(3)}$ susceptibility is associated with the refractive index of material and the imaginary part is associated with the time or phase delay in the response of the medium. The real part of the susceptibility contributes to SPM, XPM and FWM and the imaginary part contributes to SRS and SBS [56].
Non-linear effects such as SPM and XPM can be described as an intensity dependence of the refractive index and, e.g., influence the propagation of ultrashort pulses with high peak power. SPM refers to a self-induced phase shift experienced by an optical field during its propagation and leads a spectral broadening of ultrashort pulses. XPM describes the non-linear

phase shift of an optical field, however, induced by another field at a different wavelength propagating simultaneously in the fiber [57]. FWM involves parametric interaction of two or more light waves at different frequencies and can lead to energy transfer between these waves [58]. The second class of nonlinear effects, SRS and SBS results from stimulated inelastic scattering in which the optical field transfers part of its energy to the non-linear medium, in the form of vibrational excitation modes (phonons) in the medium. The main difference between the SRS and SBS is that optical phonons participate in SRS, while acoustic phonons participate in SBS [59, 60, 55].
During amplification of light from narrow line-width CW oscillators in a fiber, the non-linear effects observed are mainly due to SBS. The reason for this is that the threshold power of SBS is lower compared to the other non-linear effects mentioned above [61]. Thus, in the following section, we concentrate on the effect of SBS in fiber amplification, while neglecting the other $\chi^{(3)}$ and higher order non-linearities.

2.4.1 Stimulated Brillouin scattering

SBS is a non-linear process that occurs in fiber amplifiers, when the line width of the injected signal radiation is narrower than the SBS bandwidth which is determined by the damping of acoustic waves in the medium (in silica typically between 10-100MHz) [61]. SBS manifests itself through the generation and amplification of a backward propagating wave known as Stokes wave, whose frequency is down-shifted from the incident signal by an amount set by the non-linear medium. The SBS process exhibits a threshold-like behavior and once the threshold is reached this can lead to a significant power conversion from the signal to the Stokes wave. This limits the amplified signal power. In addition, as SBS arises from noise (i.e the thermal excitation of phonons), this can lead to significant amplitude instabilities of the amplified signal [62]. Hence SBS is highly undesirable

during amplification. Here, we will describe the physical process behind SBS and the properties of the Stokes wave such as the typical line-width and frequency shift of the Stokes wave generated from the signal wave. We discuss the typical threshold and gain associated with the SBS process for the case of passive (non-doped) fibers and we roughly estimate the SBS threshold power for active fibers. We do not attempt a numerical modeling of the SBS process, because this is quite involved and, more importantly, requires highly detailed knowledge of many fiber parameters which are often not known [63, 64]. However, we qualitatively address the factors influencing the onset of pulsing in these fiber amplifiers and present possible ways to suppress such pulsing.

Physical process

SBS can be described as a non-linear interaction between the signal and the Stokes field through an acoustic wave as illustrated in Fig 2.11. Initially, the signal field generates an acoustic wave through the process of electrostriction [51]. That acoustic wave, in turn, modulates the refractive index of the medium. The latter results in an index grating, which propagates through the medium with the speed of the acoustic wave and which scatters the signal light through Bragg diffraction. The scattered light is downshifted in frequency because of the Doppler shift associated with the movement of the grating at the acoustic velocity v_A.
The Stokes wave interferes with the forward propagating signal and generates an optical grating pattern, whose velocity and spatial periodicity matches with the velocity and wavelength of the acoustic wave. Finally, electrostriction through that fringe pattern amplifies the acoustic wave which further enhances the signal-Stokes conversion rate. This process becomes self-sustaining beyond a certain threshold power.
Quantum-mechanically, the described process can be viewed as an annihilation of forward-propagating signal photons which create back-propagating Stokes photons and forward-propagating acoustic phonons simultaneously.

As both energy and the momentum must be conserved during each scattering event the frequencies and wave vectors of three waves are related by

$$\Omega_B = \omega_{signal} - \omega_{Stokes} \tag{2.10}$$

$$\overrightarrow{k}_B = \overrightarrow{k}_{signal} - \overrightarrow{k}_{Stokes} \tag{2.11}$$

where ω_{signal}, ω_{Stokes} and Ω_B are the frequencies of signal, Stokes and the acoustic waves respectively, and where $\overrightarrow{k}_{signal}$, $\overrightarrow{k}_{Stokes}$ and $\overrightarrow{k}_B$ are the respective wave vectors. The frequency and the wave vector of the acoustic wave Ω_B and $\overrightarrow{k}_B$ satisfy the standard dispersion relation

$$\Omega_B = v_A \left|k_B\right| \approx 2v_A \left|k_{signal}\right| \sin(\theta/2) \tag{2.12}$$

where θ is the angle between the signal and Stokes fields, and $|k_{signal}| \approx |k_{Stokes}|$ is used in Eq(2.11). Eq(2.12) shows that the frequency shift of the Stokes wave depends on the scattering angle θ. In particular, Ω_B is maximum in the backward direction ($\theta = \pi$) and vanishes in the forward direction ($\theta = 0$). Thus, in single-mode fibers, where the only possible directions of light propagation are forward and backward, one observes only backward scattering of the Stokes. In this case, the frequency difference between the signal and Stokes waves is also called Brillouin shift, and is given by

$$\nu_B = \Omega_B/2\pi = 2nv_A/\lambda_{signal} \tag{2.13}$$

Here Eq (2.12) was used with $|k_{signal}| = 2\pi n/\lambda_{signal}$ and n is the modal index at the signal wavelength λ_{signal}. It can be seen from Eq(2.13)that the Brillouin shift decreases with increasing signal wavelength. When looking at numbers for silica fibers [61] one finds $v_A = 5.96km/s$ and n=1.45 which gives a Brillouin shift of $\nu_B \approx 16GHz$ at $\lambda_p = 1.08\mu$m.
Even though Eq(2.12) predicts correctly that stimulated Brillouin scattering should occur only in the backward direction in single-mode fibers,

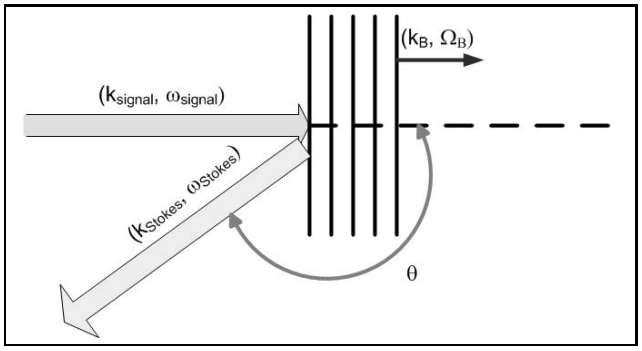

Figure 2.11: Schematic illustration of SBS process. The signal wave $(k_{signal}, \omega_{signal})$ is inelastically scattered by a mobile acoustic grating(k_B, Ω_B) and gives rise to a Stokes wave$(k_{Stokes}, \omega_{Stokes})$.

spontaneous Brillouin scattering can occur in forward direction. This happens because, in fibers, thermally excited acoustic waves are guided also in the forward direction and develop higher amplitudes than, e.g., in bulk crystals. This phenomenon is referred to as guided-acoustic-wave Brillouin scattering [65].

Brillouin gain and Threshold

The growth of the Stokes wave is characterized by a Brillouin gain coefficient $g_B(\Omega)$ that shows a Lorentzian spectral shape, with the peak value centered at the frequency of the acoustic phonons Ω_B . The spectral width of the gain spectrum is related to the lifetime of the acoustic phonon and varies from 10MHz-100MHz. The peak Brillouin gain of bulk silica is $g_p \approx 5 \times 10^{-11} m/W$ [61]. The gain depends on the ratio of signal bandwidth to Brillouin bandwidth and its spectral shape is given by

$$g_B = \left\{ \frac{1}{1 + \Delta\nu_{signal}/\Delta\nu_B} \right\} g_p \tag{2.14}$$

where $\Delta\nu_{signal}$ and $\Delta\nu_B$ are the signal and Brillouin bandwidth, respectively. The Brillouin gain attains its maximum value for $\Delta\nu_{signal} \ll \Delta\nu_B$,

i.e., for narrowband light, and the gain decreases with increasing signal bandwidth.

As seen from the small value of g_B, for development of SBS a substantial interaction of signal and the Stokes waves is required. However, it is possible, to find substantial SBS for the case of relatively low power CW or quasi-CW beams in a fibers because here the beams are tightly guided (high intensity) and long interaction lengths are present. When the signal bandwidth is smaller than the Brillouin bandwidth, $\Delta\nu_{signal} \leq \Delta\nu_B$, the growth of the Stokes wave and the depletion of the signal wave through SBS is governed by a set of coupled differential equations which, under steady-state conditions, is given by [61].

$$\frac{dI_{signal}}{dz} = -g_B I_{signal} I_S - \alpha I_{signal}, \tag{2.15}$$

$$\frac{dI_S}{dz} = -g_B I_{signal} I_S + \alpha I_S \tag{2.16}$$

Here I_{signal} and I_S are the signal and Stokes intensity, respectively, and α represents fiber loss, assumed to be same for the signal and Stokes wave. The back-propagating Stokes wave grows from noise (spontaneous Brillouin scattering occurring throughout the fiber [66]) or electrostriction from the signal wave as described above. The Brillouin threshold occurs at a critical signal power given by [55]

$$P_{th} \approx \frac{21A}{g_B L} \tag{2.17}$$

where L and A are the length and core area of the fiber. Eq (2.17) shows that the SBS threshold can be increased by using fibers with large core area and shorter lengths. It can further be seen from Eq (2.14) that the gain decreases when the signal has a bandwidth broader than the Brillouin bandwidth, which implies a higher SBS threshold for broadband light via g_B Eq (2.17). Basically, by either decreasing the fiber length or increasing the fiber area, the parametric interaction strength of the three waves is reduced, via lowering of the spatial overlap and the interaction length of the optical waves. By broadening the spectral width, the spectral overlap

between the signal and the acoustic waves is reduced. Eq (2.17) predicts the threshold for passive fibers with reasonable accuracy. To give an example, Eq (2.17) predicts a threshold power of around 1W, for a 30m long fiber, with a core area of $78\mu m^2$.

However, the threshold power is different for active fibers for a number of reasons. A main reason is that a doping of fibers changes their acoustic properties, as does a change in fiber crosssection, such as in cladding pumped fibers [67]. In addition, strain and temperature variations along the fiber length can also broaden the Brillouin gain spectrum, thereby reducing its peak value [68, 69]. Such strain and temperature variations are present during amplification. Particularly, a pump power temperature gradient is introduced throughout the fiber when end pumping of the fiber with high power diodes[70]. Moreover, inhomogeneities in fiber core crosssection along the fiber length can affect the gain and such inhomogeneities are specific for each individual fiber. As a result one finds large variations in the Brillouin gain bandwidth varying from approximately 10-100MHz in silica fibers.

To obtain a better estimate of the strength of Brillouin effects in fibers, it is useful to compare them to the results of studies on similar fibers published in the literature. A 30 m long Nd-doped fiber amplifier with a core diameter of 11μm and when amplifying a signal with a bandwidth of less than 1MHz showed an SBS threshold of 5.5W [71]. A 50m Ytterbium doped fiber with a core diameter of 8μm and a cladding diameter of 225μm showed a threshold of 2W [62]. Brilliant et al. suggested a threshold of a few Watts for single-frequency, single-mode fiber amplifiers over a length of tens of meters [62]. However, the SBS threshold values are difficult to compare directly with the results presented in this thesis, since the fiber geometries, the dopants, and dopant concentrations are different, which all influence the SBS threshold. We use a Ytterbium doped fiber which has a 10μm core and a 400μm D-shaped inner cladding with lengths of 36m and 50m. From these data, we estimate the threshold of our Ytterbium-

doped fiber amplifier to be in the order of 5W to 10 W, in which we have neglected an influence of compositional variation of the core material or built-in strain. Similarly we estimate a Brillouin bandwidth in the range of 10-100MHz and the Stokes shift to be around 10-20 GHz, at a signal wavelength of 1.06μm.

2.4.2 SBS dynamics: pulsing and their suppression

When the signal power exceeds the SBS threshold, the Stokes and signal waves can exhibit a strong temporal variation seen as intense output pulses in both the propagation directions. This pulsing observed at the Stokes wave grows at the expense of the signal. A theoretical description of the corresponding temporal dynamics is extremely complex because it has to include a time dependence of the signal and Stokes waves into Eq(2.15) and Eq(2.16), and one also has to include the optical gain provided by population inversion in the fiber [72, 73], possibly even residual feedback from the facets of the fiber. Here, we restrict to a qualitative discussion of these factors influencing the pulsing observed in our fiber amplifiers and rather provide experimental ways to suppress this pulsing.

There is extensive work in literature, describing the named pulsing in active fibers. However, a clear physical picture remains missing, because the observations seem to depend very much on the particular case investigated. In certain cases, the generated Stokes pulses have been found to be periodic, with the frequency of round-trips in the fiber[74, 75]. Boyd et al. have shown the initiation of the SBS from noise via thermal fluctuations leading to a stochastic behavior of these pulses [66, 76]. Even a chaotic behavior of the Stokes pulses has been reported [77, 78]. In a simple picture, the generated SBS Stokes wave can experience gain available in the fiber, with the fiber-amplified spontaneous emission (ASE) seeding the Brillouin scattering in both the directions and both the signal and Stokes wavelengths. Moreover, a large fiber gain can lead to generation of multiple order Stokes lines [63]. Here, the first order Stokes wave acts as a signal for the second

order Stokes wave generated in the direction of the signal wave [64]. Thus, ASE can also induce pulsing and saturate the amplified signal output in fiber amplifiers. A fiber with broad gain bandwidth, when used for amplifying signals with low power or for a signal wavelength far away from the maximum of the gain spectrum, can lead to pulsing at non-signal wavelengths due to unsaturated gain. This can be prevented by saturating the amplifier with sufficient signal power and by choosing the operating signal wavelength closer to the gain maximum of the fiber.

From a practical point of view the growth of the Stokes power in the backward direction along the length of the fiber is unwanted in amplifiers, as this limits the amplification of the signal wave because the Stokes wave depletes the inversion as well [71, 62]. Thereby the Stokes pulses can develop high peak power, particularly in high power amplifiers, where the signal power easily increases beyond the SBS threshold. The backward propagating high peak power Stokes pulses can be also be detrimental to the signal oscillator source. Here, they can lead to spectral and power instabilities and sometimes even destroy the signal source. In addition, these pulses can also damage the fiber facets, where the damage threshold is lower than within the fiber. All this, is highly undesirable during the amplification process [62]. It is thus important to look for ways to suppress such pulsing, by identifying and controlling the factors governing the SBS threshold.

From Eq(2.17) and Eq(2.14), we recall that the threshold power for the SBS process depends on three parameters namely the fiber core-area (i.e., its diameter), the fiber length, and the bandwidth of signal source. However, increasing the core area can lead to propagation of higher order signal modes. Shortening the length of the fiber also is no interesting option, because this would reduce the absorption of pump light in the fiber and thus lower the amplification efficiency and output power. Here one could try to increase the doping concentration during fabrication of fibers, as long as this does not dis-improve the basic spectral properties described in Section 2.3.2. A broadening of the signal spectral bandwidth in a controlled way

looks promising for suppression of the pulsing. Here we mention another point of practical interest having to do with the observation that pulsing often occurs with a repetition rate involving the round-trip time in the fiber [74, 75, 66, 76]. This indicates that residual feedback from the fiber facets also reduces the threshold for SBS, such that self-pulsing can occur at lower powers [62, 79]. External feedback can normally be prevented by the use of isolators and AR coated components, while preventing internal feedback from the fiber facets is more difficult, as it requires high quality and properly cleaved facets (typically at least 8 degrees) [71].
The SBS threshold dependence on the the fiber length and core area have recently led to the development of a new large mode area (LMA) fiber technology, resulting in LMA fibers with an increased core diameter and a slightly reduced index contrast between the core and the inner-cladding [80]. The larger core diameter provides a better spatial overlap with the pump light guided in the inner-cladding, which enables shorter pump absorption lengths. This allows for shorter fiber lengths without loss of pump absorption and results in a higher SBS threshold. Prior to this development, the threshold power of SBS in a typical fiber amplifier as cited by Zawischa et al., with a 30m long Nd-doped fiber and a core diameter of 11μm, for single-frequency signal radiation, was 5.5 W [71]. With LMA fibers, amplification of single-frequency signal radiation up to 108W was obtained before the onset of SBS in an Yb-doped fiber with a core radius of 28μm and length of 9.4m [48]. However, although the reduced index contrast reduces the V-parameter the increased core diameters still enables multi (transverse) mode propagation, which reduces the spatial quality of the output from the fiber amplifier. To still ensure single-mode propagation, a heuristic approach is to tightly coil the fiber, thereby attempting to induce higher propagation losses to the higher order modes than to the fundamental mode, although this does lead to stress-induced birefringence. A major disadvantage of LMA fibers with too large a core is that the signal power needed to saturate the fiber gain is much higher (typically hundreds of mW

to Watt-levels) than with a smaller core. Typical diode oscillators designed for excellent spectral and tuning properties offer an output power in the mW-range and would thus not be able to saturate an LMA fiber amplifier with a larger core.
In view of these arguments we believe that the best compromise for a diode-oscillator fiber-amplifier system is to choose an LMA fiber, but with its core size at the smaller side. This way we expect that the fiber output is still well sufficient to drive an SRO, while the required seed power (from the diode oscillator) remains in the mW-range. Therefore for all works described in this thesis, we chose an LMA fiber with a core size of 10μm.
In chapter 3, we experimentally investigate the suppression of power instabilities seen as a pulsing of our Ytterbium doped fiber amplifier by specifically focusing on a suppression of pulsing via a controlled spectral broadening of the injected signal to be amplified. This way, the pulsing in the fiber amplifier is suppressed to obtain stable multi-Watt-level output with less than 1% variation measured over hours.

2.5 Summary

In this chapter, we have given a brief review of various important aspects that would play a role in mid-IR generation based on a diode-oscillator Yb-fiber-amplifier combination followed by an SRO. In section 2.1, we discussed the operation principle and the various tuning options for OPOs. We outlined the advantage of SROs (vs DROs and TROs) for providing an easy, wide, and rapid tuning in the mid-IR, and we stated the requirements that are imposed on the pump laser source, for applying a pump-tuning of SROs.
In section 2.2, in view of these requirements, we have compared the various different pump laser sources that have been used so far for SRO operation. We conclude that a diode-oscillator fiber-amplifier pump laser systems appears most promising because this combines the advantageous spectral and

tuning properties of diode lasers with the high-power capabilities of fiber amplifiers.

In section 2.3 we reviewed the properties of double-clad Ytterbium doped fiber amplifiers, because these appear most suitable for corresponding experiments. We discussed the benefits of employing such double-clad fibers over single-clad fiber amplifiers with regard to the higher powers that can be achieved.

In section 2.4 we discussed the drawbacks of these double-clad fiber amplifiers manifesting as power and frequency instabilities arising from non-linear effects, in particular through SBS, when amplifying light of narrow spectral bandwidth. We discussed the various factors that enhance such instabilities, such as feedback and ASE, and we suggested to employ a spectral broadening of the signal wave to be amplified for suppressing these instabilities.

Chapter 3

General characterization of Ytterbium-doped fiber amplifier

Real time detection of trace gases requires widely and rapidly tunable mid-IR light sources. In addition, such sources should satisfy requirements such as narrow spectral width of the order of 100MHz-500MHz, enough to resolve the spectral lines of the envisioned trace gas molecules, and it should provide a stable output and high average power for sensitive detection. We have discussed in the previous chapter that a pump-laser-tuned, singly resonant OPO (SRO) looks promising to realize such a wide and rapid wavelength selection in the mid-IR region, because these SROs essentially down-convert all spectral properties of a near-IR pump laser, such as spectral width and tuning properties. From this we conclude that it is important to devise and investigate near-IR pump lasers, which can satisfy the requirements regarding the spectral width and the wavelength tuning and that diode oscillator based pump sources would be most promising for this task. Diode lasers offer only low power in the milli-Watt range, which is about 3 orders of magnitude below what is the typical threshold of an

SRO. However, these low output powers can be overcome when amplifying the diode output in a suitable power amplifier. The power amplifier should offer the following properties:

1. Amplification over three orders of magnitude in power, from the milli-Watt level to the multi-Watt level, sufficient for operating an SRO well above its threshold of typically several Watts.

2. Stable output power at a spectral width of the input radiation below 100-500MHz to reliably resolve and identify the mid-IR spectral lines.

The recent advances in the field of fiber technology with respect to high powers have led to our choice of optical fibers as suitable amplifiers. Meanwhile fiber amplifiers have many advantages compared to bulk solid-state amplifiers. Fiber amplifiers are free of the thermal problems encountered in traditional bulk solid-state amplifiers. Fiber amplifiers have a broad amplification gain bandwidth and are typically more efficient than the bulk amplifiers. In double clad fibers, pump conversion efficiencies as high as 80% have been reported across a broad gain bandwidth [45]. Light amplification in these fibers is often limited only by the available pump power and the onset of non-linear effects. With the availability of high power pump diodes, power levels over 264 W output at a single frequency [49] and up to kilo-Watt power levels with multimode output have been achieved with these fibers [50]. However, as discussed in chapter 2, when amplifying rather narrow line width laser sources ($< 100MHz$), undesired non-linear effects such as stimulated Brillouin scattering (SBS) hamper the amplification process [71]. More specifically, the build-up of a Stokes wave along with fiber feedback from fiber facets and non-depleted gain can lead to regular, stochastic or chaotic pulsing in fiber amplifiers, which limits amplification of the signal wave [62]. In chapter 2, it was suggested that pulsing can be suppressed, among other methods, by a broadening of the signal bandwidth [81, 82]. Hence, it is important to investigate the amplification

of radiation from diode laser oscillators, because these can easily be broadened spectrally in a controlled manner, via a direct current modulation of their pump current.
In this chapter we experimentally characterize the amplification of DBR diode laser radiation in two Ytterbium-doped double-clad fiber amplifiers and we investigate the suppression of pulsing during amplification via a controlled spectral broadening of the diode laser output. Thereby, we obtained stable multi-Watt output power. In the following we describe the experimental setup of the diode-laser fiber-amplifier setup and present experimental data on the maximum stable amplified output obtained by suppression of the pulsing.

3.1 Experimental setup

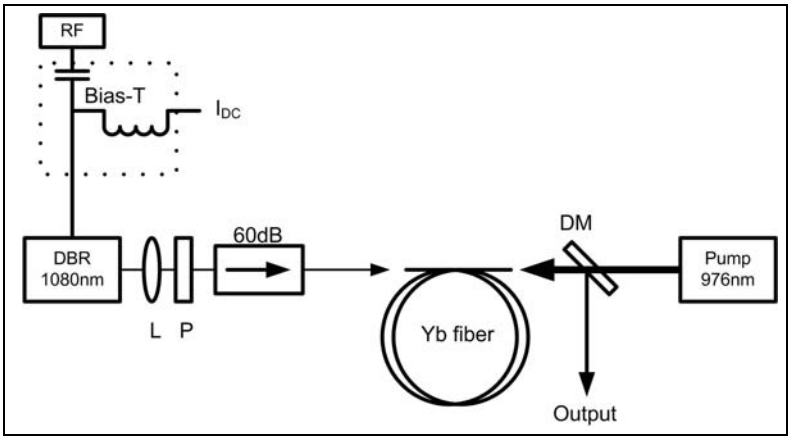

Figure 3.1: The experimental setup of the DBR diode laser fiber amplifier system. RF: RF signal generator, DBR: DBR diode laser, L: collimating lens, P: half-wave plate, Yb fiber: Ytterbium-doped fiber, DM: dichroic mirror, Pump: 25W pump diode

Fig 3.1 schematically shows the setup consisting of two stages: a master-

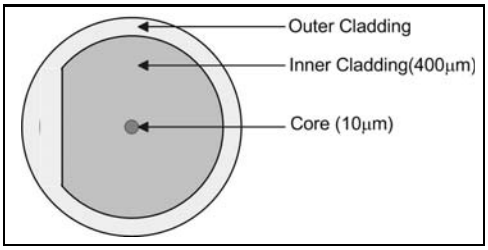

Figure 3.2: Schematic illustration of the double clad fiber cross section, Core: Yb-doped fiber core where the signal propagates, Inner-cladding: D-shaped cladding where the pump light propagates, Outer-cladding: Circular cladding which restricts the pump light to the inner cladding.

oscillator based on a DBR diode laser[1] and a power-amplifier based on an Ytterbium-doped fiber. Without a modulation of the pump current, the bandwidth of the DBR laser was measured to be less than 30MHz, for which a scanning confocal Fabry-Perot interferometer was used with a free spectral range of 3GHz and a resolution bandwidth of 30 MHz. The DBR laser is temperature stabilized at $20°C$ and is driven with a DC current up to 120 mA in continuous wave operation with a home-made diode laser driver. The laser has a threshold current of 30 mA, emits at wavelength of 1080 nm and produces a maximum output power of 50 mW. The beam from the DBR diode laser is collimated (Thorlabs C230TM-B, f=4.5mm, N.A=0.55) and focused through a polarization controller and two Faraday isolators, which provides a 60 dB suppression for the radiation generated from the amplifier in the backward direction towards the DBR oscillator. During measurements the diode laser power injected into the fiber amplifier (seed power) was varied by controlling the polarization before the isolator via rotation of the half-wave plate, whereas the diode was operated with a fixed drive current. This ensures that the seed wavelength does not change. The home made diode driver can also be used for direct current modulation for frequencies up to 3MHz. For higher modulation frequen-

[1] Manufactured by Eagleyard Photonics GmbH, Berlin, Germany

cies, an RF current (<1mA) generated from a function generator (Voltcraft FG-513) is superimposed on the DC current via an bias-T (Mini circuits-ZFBT-4R2GW operating range: 0.1-4200MHz). For all the measurements presented in this chapter, except when the effect of modulation frequency on the pulsing threshold is studied, the diode laser is modulated using a 3MHz sinusoidal wave and the spectral bandwidth of the laser is increased via an increase of the modulation current amplitude.

The power amplifier is based on a large mode area (LMA) double clad Ytterbium-doped fiber[2]. The active core has a diameter of 10 μm and a numerical aperture (NA) of 0.07. The core is Ytterbium-doped at a concentration of 1000 mole parts per million. The core is surrounded by a D-shaped inner cladding (shown in Fig 3.2) with a 400 μm diameter and an NA of 0.38, which is end-pumped at the signal output side by a fiber-coupled (400 μm diameter and NA 0.22) broad-band diode laser at 976 nm. The maximum pump power available from this pump diode is 25W. The fiber facets were cleaved with a fiber cleaver (FK11-Precision fiber cleaver). Approximately 75% of the pump power was launched into the double clad fiber, which was measured using short fibers ($\leq$ 30 cm), in which pump absorption can be neglected.

The diode laser output (signal) is amplified in two alternative pieces of fiber having a length of 36 m and 50 m. A dichroic mirror separates the amplified signal output from the pump input. A fast silicon photodiode is used to monitor the power stability of the amplified output. An optical spectrum analyzer (ANDO type AQ6317) with 0.015 nm resolution (4 GHz at 1060 nm) is used to monitor the spectrum of the amplified signal radiation and to evaluate the background of amplified spontaneous emission (ASE). The output power measurements are performed with a calibrated power meter (Newport, thermopile 1815C).

[2]Manufactured by IPHT Jena, Germany

3.2 Experimental results

In our measurements we observed that, at a given signal power, the power of the amplified output signal from the fiber amplifier initially increases, when the pump power is increased. However, when the bandwidth of the signal is too narrow, self pulsating occurs before the amplifier is pumped at the maximum available pump power. With the onset of pulsing behavior, the average amplified output remains constant, i.e., it does not increase further with the pump power and, instead, there is an increase in the Stokes power generated by SBS in the backward direction. In our experiments, we have recorded the pulsing threshold, i.e., the maximum pump power and corresponding output power, before pulsing as a function of the DBR diode laser bandwidth and the DBR diode laser input(seed) power.

Effect of signal power and bandwidth on pulsing threshold

Fig 3.3 shows the maximum stable output power measured behind the fiber amplifier as a function of the diode seed power, while the seed signal bandwidth was increased in steps of 30MHz to 250MHz via the diode modulation current. From Fig 3.3a and Fig 3.3b it can seen that, for a given laser bandwidth, the maximum amplified stable output increases with the seed power for both the fibers. The lower pulsing threshold at lower seed powers can be due to the combined effect of unsaturated gain and SBS in the fiber as was discussed in chapter 2.
It can be seen that the maximum available diode seed power of 35 mW can be amplified up to 5.5 W and 7.8 W, when the bandwidth is narrow (30MHz) before the pulsing sets in for the 50 m and 36 m fiber, respectively. When the seed radiation is broadened spectrally, by an increasing modulation current, the threshold for pulsing increases, until the amplifier

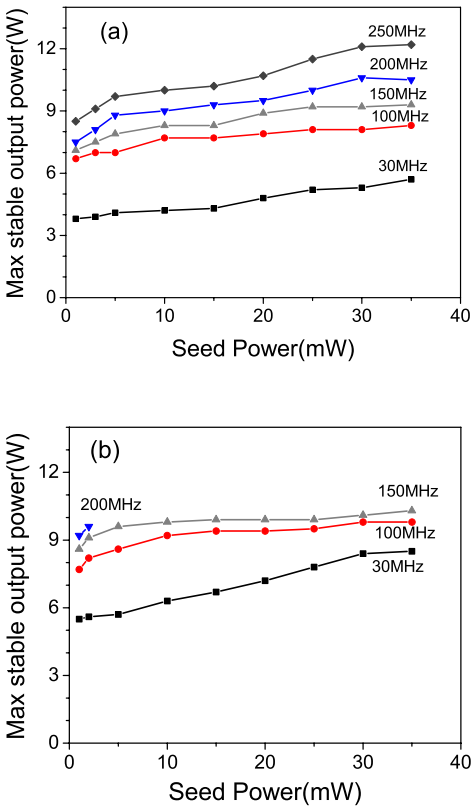

Figure 3.3: The maximum stable output power as a function of seed power of the signal for various signal bandwidths. (a) 50m long fiber (b) 36m long fiber.

output is limited only by the available pump power of 25W. In this case, a maximum amplified stable output of around 12 W was achieved with 250 MHz seed laser bandwidth in the 50 m fiber, and it is around 10 W with 150 MHz bandwidth in the 36 m fiber. The maximum amplified output power showed less than 1% power residual variation over many hours of continous operation for both the fibers.

In order to determine the slope efficiency of the two fiber amplifiers, the

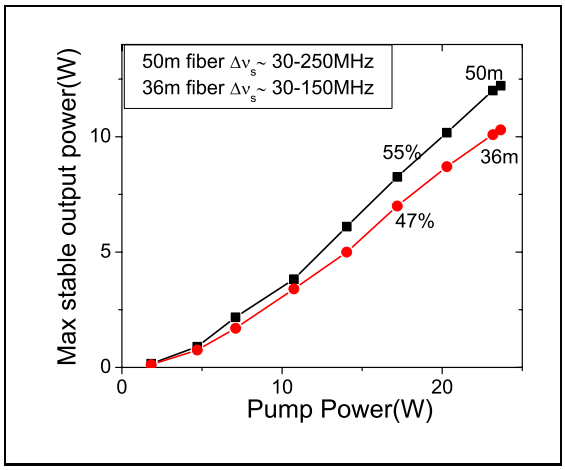

Figure 3.4: The maximum stable amplified signal output as a function of the pump power launched into the fiber, achieved by suppression of pulsing behavior in the 36m and 50 m fiber, by an increasing signal bandwidth $\Delta\nu_s$.

data points from Fig 3.3 recorded with maximum seed power (35mW) were replotted as shown in Fig 3.4. It can be seen that the slope efficiency is 55% and 47% for the longer and shorter fiber, respectively. The output power and pump conversion efficiency for the 50m fiber was higher because in this fiber more pump light is absorbed due to its larger length.
From Fig 3.3 and Fig 3.4 it can be seen that suppression of pulsing requires a different amount of spectral broadening in the two fibers, namely, pulsing in the shorter fiber is suppressed with less broadening (150MHz instead of 250MHz). The SRO pump laser requirements described earlier set a 100 MHz-500MHz upper limit on the bandwidth. At the lower end of this range, i.e., at a bandwidth of 100 MHz, the 50 m fiber produces a stable output of around 8 W compared to over 9 W produced in the 36 m fiber. The higher amplified power at the required bandwidth led to our choice of the 36 m long fiber for our further experiments.

Modulation parameter limits for stable operation

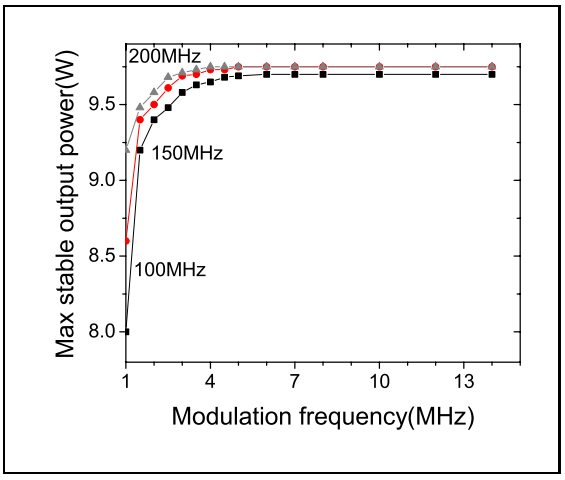

Figure 3.5: The maximum stable output power as a function of the modulation frequency for various signal bandwidths for the chosen 36m fiber.

While the above results show that spectral broadening by modulation of the seed laser can be used to suppress unwanted pulsing in the amplifier, it is important to establish the limiting values of the various modulation parameters if stable operation is to be reliably achieved. For example, it would be useful to know what minimum spectral bandwidth must be used at a given modulation frequency or whether the bandwidth required can be reduced by increasing the modulation frequency.
Fig 3.5 shows the maximum amplified stable output achieved with the 36m fiber, as a function of modulation frequency, for three spectral bandwidths (i.e., three modulation amplitudes). It can be seen that almost the same maximum output power of approximately 9.6W was achieved for all bandwidths once the modulation frequency is beyond 4MHz. Thus, there is little to be gained by increasing the modulation frequency further. For modulation frequencies below approximately 3MHz, achieving higher sta-

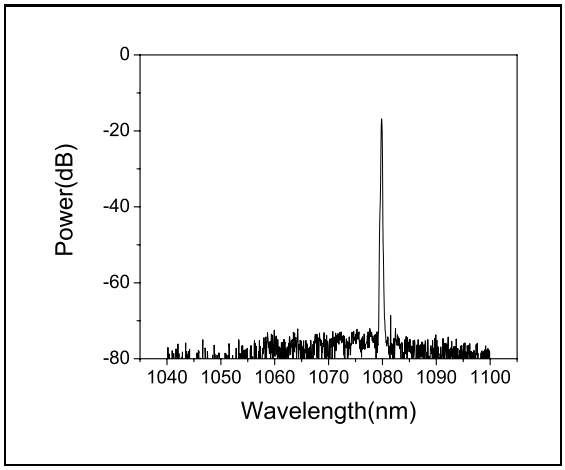

Figure 3.6: Optical spectrum analyzer output shows a 50 dB background suppression at maximum amplified output.

ble output powers required an increased bandwidth (i.e., modulating with greater amplitude), although the effect was small. Therefore, a modulation frequency of 3MHz should generally be used to achieve the highest power with minimum overall bandwidth.
Finally Fig 3.6 shows the spectrum of the amplified radiation as measured with the optical spectrum analyzer (OSA). It can be seen that, at the maximum amplified output of around 10W, the ASE background is suppression by more than 50 dB with regard to the amplified signal. This shows that almost all of the output power is concentrated at the signal wavelength of 1080nm and the contribution from ASE can be neglected.

3.3 Summary

To summarize, the output from a narrow bandwidth DBR diode laser was amplified in two Ytterbium-doped fiber amplifiers of length 36 m and 50 m. A maximum stable output power of 10 W and 12 W was obtained, re-

spectively, by suppressing the pulsing in both the fibers. This was achieved by current modulating the DBR diode laser, which leads to broadening of its spectral bandwidth. The pulsing threshold was recorded as a function of seed laser power and bandwidth for both the fibers. The 36 m long fiber was chosen ahead of the 50 m long fiber for our further amplification experiments, as the maximum stable output produced was higher at lower bandwidths. For instance, a maximum of over 9 W output was produced using the 36m fiber amplifier at a bandwidth of 100MHz, which is well sufficient to operate an SRO and produce mid-IR radiation to resolve mid-IR molecular absorption lines. The amplified output was stable over several hours of continuous operation, with a power variation of less than 1%, and the ASE background was suppressed by more than 50dB at a seed input power of 35mW.

Chapter 4

Spectral shaping of a 10W diode laser-Yb-fiber amplifier system[1]

In the last chapter, we described the advantage of employing a diode laser as a seed source for a fiber amplifier, where a weak modulation of the diode laser was used to suppress SBS related self-pulsing of the fiber during amplification. In this chapter, we investigate the effect of much stronger modulation on the diode laser spectrum and its applications. Here, we describe a continuous-wave (CW) master-oscillator power-amplifier (MOPA) system based on a DBR diode laser and an Yb-doped fiber amplifier. The observed optical spectrum of the amplified seed source can be tailored to arbitrary shapes and over GHz widths, by controlling the radio frequency (RF) modulation waveform of the injection current [83]. The spectrally-tailored output of the diode laser is amplified to a multi-Watt level in a 36m long Ytterbium-doped fiber amplifier.

This chapter is organized as follows. Section 4.1 introduces the need for

[1]Published as: B.Adhimoolam et al, Rev. Sci. Instrum., **77**, 093101-1– 093101-4, 2006

arbitrarily shaped spectra with high powers and the advantage of fiber amplifying an arbitrarily shaped spectral output of a DBR diode laser in realizing this will be discussed. The detailed experimental setup consisting of the multi-section DBR diode laser and an Ytterbium-doped fiber amplifier will be presented in the section 4.2. This is followed by the experimental results, where the spectral results of the diode laser modulated by different waveforms and the output power measurements after amplification in a fiber are presented in the section 4.3. Finally we conclude the chapter by a brief summary.

4.1 Introduction

Vast improvements in the output power and the spectral properties of the diode laser over the past decades have led to their choice over other laser types for various applications. One such application is the field of optical pumping. Of particular relevance to this work is the spin-polarization of ^{3}He achieved with pumping at around 1080 nm [84, 85], used in medical applications (nuclear magnetic resonance tomography) or application as neutron spin polarizer, both of which require the excitation of large volumes (liters) with maximum efficiency. Transitions induced between the $2^3S - 2^3P$ states of helium, when driven with, for e.g., circularly polarized light, induces a partial polarization of the nuclei of metastable atoms. Subsequent collisions these metastable atoms and ground state atoms then transfer this polarization to the $1S$ ground state, thereby creating a permanent magnetization of the gas with lifetimes over minutes. At room temperature, which is present in an optical pumping cell, the $2^3S - 2^3P$ transitions are typically Doppler broadened by 2GHz [86], and cannot be efficiently saturated with a laser when this laser has a much narrower bandwidth. The pumping efficiency has been theoretically investigated, and shown to be strongly dependent on the spectral shape of the laser line [87]. More specifically, a high-power laser source with a Gaussian line-shape is

required that matches the Doppler width. Further, when this is achieved by broadening the laser spectrum via frequency modulation, the narrow band laser has to be modulated at a frequency faster than the inverse of the lifetime of the upper state to which the atoms are pumped ($\approx 0.1\mu$s). This would ensure that all the velocity groups become saturated which results in a maximum spin-polarization [88]. In spite of this, only simple modulation has been used to demonstrate improved efficiency over pumping with narrow-band sources [84, 89, 90], although the resulting spectral distribution does not match a Gaussian profile. Several designs of all-fiber MOPA systems have been investigated to the 5-Watt-level, and high-power fiber oscillators have been investigated to the 10-Watt-level [88]. However, imposing a particular spectral shape or even an appropriate overall bandwidth, remains difficult.

In our previous work, we demonstrated a single-stage, high-power diode-fiber MOPA system, which is continuously tunable (mode-hop-free) over a range of 110 GHz [34]. However, its tuning speed (maximum a few Hz repetition) is too low in view of the lifetime argument given above. This has led to our investigation of rapid modulation of lasers generating arbitrary average spectral distributions.

In this chapter, the modulation properties of a single-stage diode-fiber MOPA system that emits Watt-level CW output power at a wavelength around 1080 nm are described. The narrow laser bandwidth is rapidly modulated with various temporal functions to produce optical spectra with various shapes. The direct current modulation of the DBR diode laser oscillator by three modulation functions: sinusoidal, triangle and an inverse hyperbolic tangent, results in spectra resembling a U-shape, a rectangle and a Gaussian, respectively. The limitations on the spectral shapes due to the effect of amplitude modulation (AM) originating from the direct current modulation of the diode laser current are also discussed.

4.2 Experimental Setup

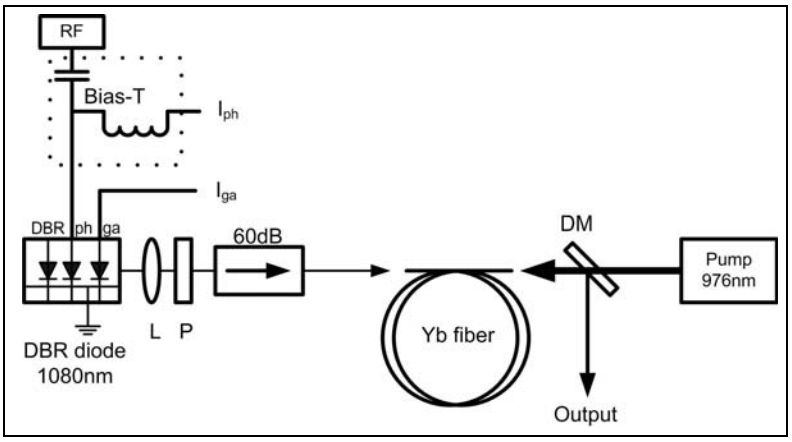

Figure 4.1: Experimental setup: DBR Diode: distributed Bragg reflection diode laser with independently controlled gain section (ga), phase section (ph) and grating section (DBR); L: collimating lens, P: half-wave plate, 60 dB: double-stage Faraday isolator with 30 dB isolation each; Yb fiber: 36 m Yb-doped double clad fiber; DM: dichroic mirror and pump diode: 25 W at a wavelength of 976 nm.

The schematic setup of the diode-fiber MOPA system is shown in Fig 4.1. The master-oscillator is a three-section DBR diode laser [1] with a threshold current of 80 mA. After passing the output of the laser through two 30 dB isolators the maximum available power is 30 mW, obtained at a drive current of 150 mA to the gain section. The structure of the diode laser [91] comprises sections for gain, phase control and DBR feedback. The latter two are fitted with resistive micro-heaters to allow thermal tuning of the output wavelength at frequencies of tens of Hertz. By simultaneous and synchronous control of the resistor currents, up to 110 GHz of continuous tuning could be achieved [34], thus providing a means to tune the center wavelength of the laser to spectral lines of interest in pumping applica-

[1] Manufactured by Eagleyard Photonics GmbH, Berlin, Germany

tions. This thermal tuning mechanism is, however, too slow to achieve the frequency modulation at MHz levels required for spectral broadening and shaping.

In normal operation, the tuning currents for the phase and DBR section heaters are derived from sources floating with respect to the anode and cathode connections to the gain section. This ensures that the tuning currents flow only through the heating resistors and the diode junction in these sections remains unbiased. However, connection of the tuning current terminals to a supply having a common ground with that of the gain section allows biasing of the phase or DBR sections in the same manner as the gain section [92]. With our device, it was found that modulation via the phase-section bias current, in this manner, could be achieved with higher bandwidths than via the gain section. To achieve this, a DC bias and high-frequency modulation currents were applied to the phase section via a bias-T (Minicircuits, ZFBT-4R2GW operating range:0.1-4200 MHz). A DC bias of 45 mA was used to ensure high-frequency modulation took place in a forward-biased, and therefore approximately linear, regime. This also had the effect of reducing the gain section current at threshold and increasing the maximum output power, after isolation, to 45 mW. The output spectrum under various modulation conditions was measured using a 3 GHz free-spectral range confocal Fabry-Perot interferometer. In the absence of modulation, a spectral width of 30 MHz was measured, limited by the interferometer resolution.

For sinusoidal modulation a signal generator (Marconi 2022) was used to provide the driving RF waveform. A fast arbitrary waveform generator (AWG 2021) was utilized to produce complex waveforms. The arbitrary waveform generator can be programmed with analytical expressions to obtain the desired waveforms. The repetition frequency of the waveform was chosen such that, after digital-to-analogue conversion (1024 pixel window with 1.024GHz clock frequency) it generated the waveform in multiples of 8, so that unwanted Fourier components are suppressed. In front of the

amplifier 40 mW of modulated output from the diode oscillator was available. The amplifier consisted of a 36 m long Yb-doped double-clad large mode area (LMA) fiber[2], as described in chapter 3. An optical spectrum analyzer (ANDO type AQ6317) with 0.015 nm resolution (4 GHz at 1060 nm), is used to monitor the amplified signal spectrum and to evaluate the signal to ASE background ratio of the amplified signal. The output power measurements are performed with a calibrated power meter (Newport thermopile 1815C).

4.3 Results-Output power and Spectral Shapes

First, the power of the amplified diode radiation as a function of pump power is measured. For these measurements the modulation waveform is an inverse hyperbolic tangent with a repetition frequency of 16 MHz and an rms current around 0.85 mA. This resulted in an average optical spectral distribution that is Gaussian in shape with a 90 MHz bandwidth (FWHM) as shown in Fig 4.2(b). Fig 4.2(a) shows that the maximum output is 10 W for a maximum in-coupled pump power of 19 W. The maximum slope efficiency is 55%. Beyond a pump power of 5.5 W, the output power increases linearly with pump power indicating that the fiber amplifier is saturated. The spectral density of amplified spontaneous emission (ASE) is suppressed by more than 50 dB with respect to the amplified diode radiation, and the total ASE power is less than 1% of the total output power as shown in Fig 4.2(b). The output power is stable over long periods of time with less than 1% fluctuation over a period of hours. This indicates that pulsing due to stimulated Brillouin scattering, common in fiber amplifiers [88], was effectively suppressed [93] by the spectral broadening achieved through modulation.

[2]Manufactured by IPHT Jena, Germany

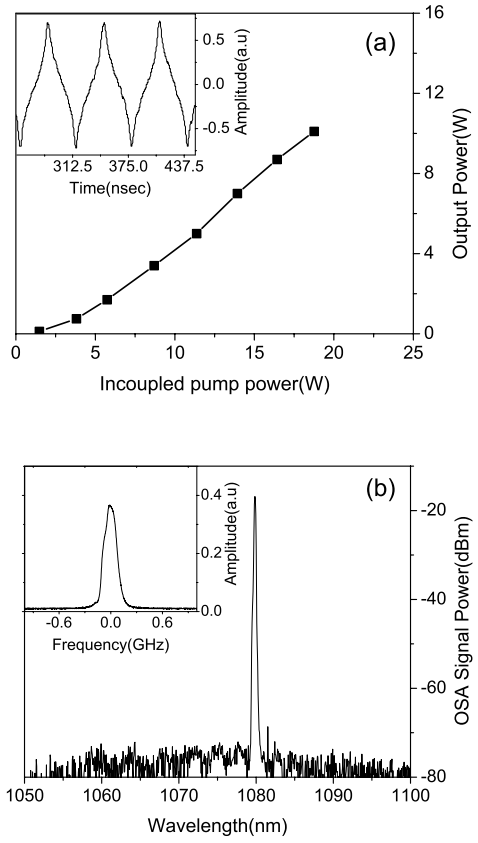

Figure 4.2: (a): Output power of the diode-fiber MOPA system vs. incoupled pump power. Inset shows the archtanh modulation applied to the DBR diode laser at ω_m(frequency) = 16 MHz; (b): Power spectrum of the amplified output showing $> 50dB$ ASE background suppression, when the MOPA system operates at maximum output power. Inset shows the Gaussian-shaped diode laser spectrum, resulting from the modulation depicted in inset (a), with $\Delta\nu_L$ =90 MHz at $I_{rf} \approx 0.85$mA.

The spectral distribution of the laser is characterized for three different

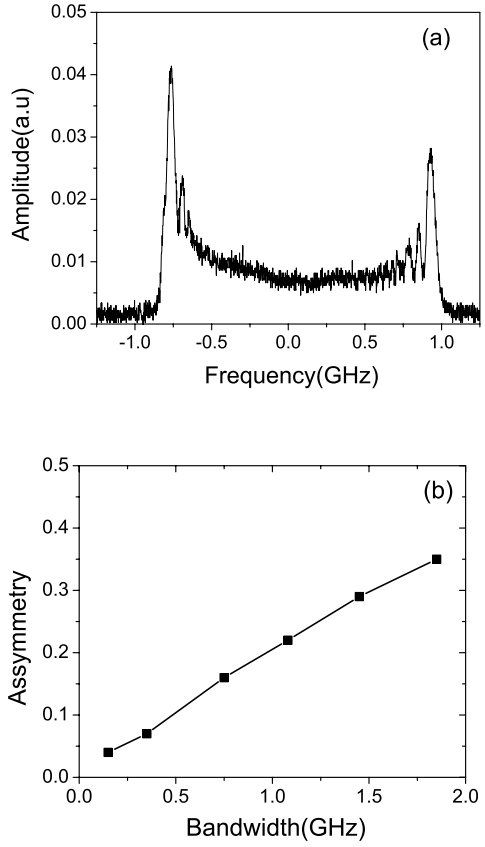

Figure 4.3: Optical spectral properties of the diode with modulation of the diode's phase section current: (a) sinusoidal modulation at ω_m= 20 MHz and I_{rf} = 7 mA. (b) The asymmetry between the peaks for sinusoidal modulation increases with laser bandwidth.

current modulation functions. When the laser is modulated with a sinusoidal function of frequency 20MHz, a U-shaped distribution is expected because the amount of time the modulation current I(t) spends in a given interval between I and I+dI (and thus the time the laser output frequency falls in the corresponding interval between ν and $\nu + \Delta\nu$) is greatest at the

extrema of the modulation current. Thus the average output power at the frequencies associated with peak and minimum current of the sinusoidal modulation function will be greatest [94]. An example of a U-shaped spectral distribution is shown in Fig. 4.3(a), in this case an rms current of 7 mA is employed and the distance between peaks was 1.8 GHz. The distance between the peaks of the spectral distribution increased by 280 MHz per mA RF current amplitude. The asymmetry observed in the spectral distribution is due to amplitude modulation of the laser output power [95]. Fig 4.3(b) shows the asymmetry between the peaks as a function of the peak separation. The asymmetry becomes larger with higher modulation currents; it is 4% when spectral width is around 150 MHz, and it increases linearly to around 35% at a spectral width of 1.8 GHz.

A rectangular spectral distribution can be achieved by triangular modulation. In this case the amount of time I(t) spends in the current interval from I to I + dI is the same for all I, so the distribution of power in the averaged spectrum should be equal for all frequencies addressed within the modulation range. Fig 4.4(a) shows a 120 MHz broad spectral distribution resulting from 16 MHz triangular modulation function with a peak current of around 0.85 mA. The influence of amplitude modulation is more significant in this case leading to asymmetric ripple in spectrum that increases with the width of the spectrum as shown in Fig 4.4(b). The best fit line to a measure of the ripple amplitude, which is a measure of deviation from the rectangular spectrum, increases linearly with spectral bandwidth at a rate of 1% per MHz to 50% at 500 MHz.

As mentioned earlier, it has been theoretically shown [94] that, modulating the diode current with an inverse hyperbolic tangent function should lead to a Gaussian spectral distribution. This can again be understood in terms of the time spent by I(t) in the current interval from I to I + dI. The inverse hyperbolic tangent changes slowest when I is near zero, thus maximum average power is emitted in the center of the spectrum. The derivative of I(t) goes to infinity at the current maxima and minima, thus

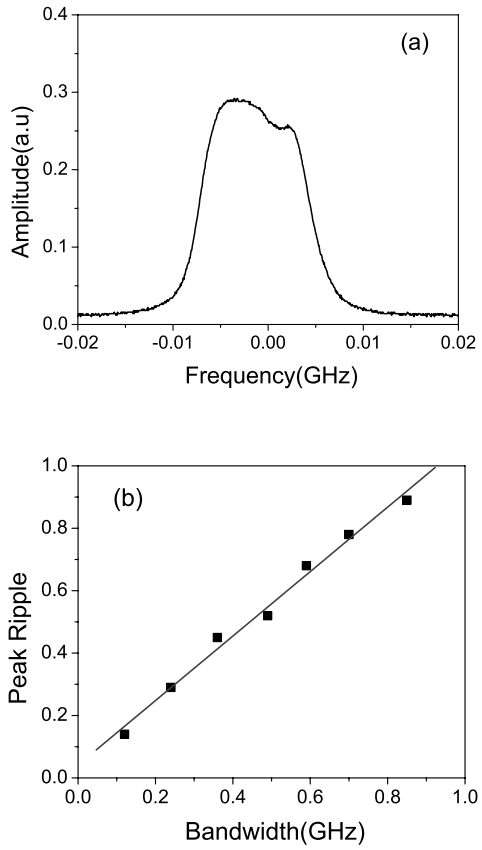

Figure 4.4: Optical spectral properties of the diode with modulation of the diode's phase section current: (a) Triangular modulation at ω_m= 16 MHz and $I_{rf} = 0.85$ mA. (b) Best fit of ripple shows linear increase for triangular modulation with laser bandwidth.

decreasing power is emitted with increasing distance from the center of the spectrum. Fig 4.5(a) shows the optical spectral distribution obtained when modulating the diode with a 16 MHz inverse hyperbolic tangent with a peak current of 5 mA along with a Gaussian fit. Again the spectral distribution is slightly distorted on one side, which can be attributed to amplitude mod-

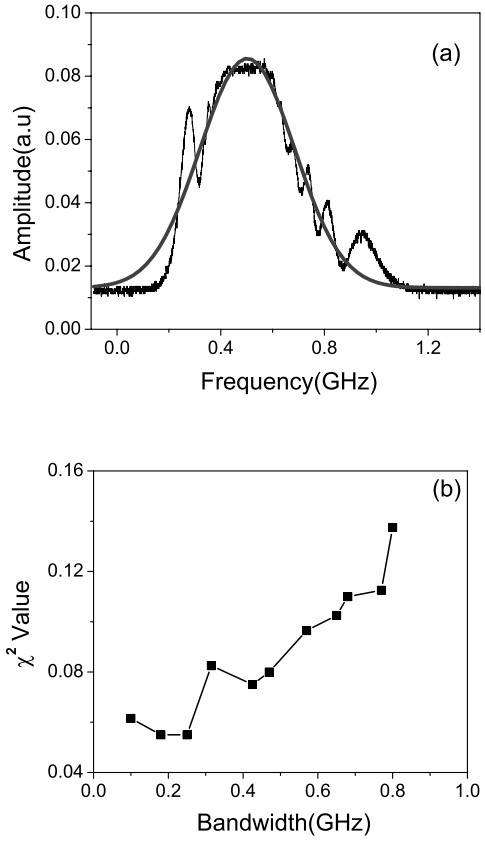

Figure 4.5: Optical spectral properties of the diode with modulation of the diode's phase section current: (a) Inverse hyperbolic tangent modulation $\omega_m = 16$ MHz and $I_{rf} = 5$ mA and (b) root-mean-square deviation from Gaussian spectrum χ^2 as a function of laser bandwidth.

ulation seen as an emerging peak. The peak grows in height with increasing modulation current. Beyond a spectral width of 500 MHz shown here, the deviation from a Gaussian is obvious. The amount of root-mean-square deviation of the experimental data from the Gaussian shape, denoted as χ^2, is plotted against the measured spectral bandwidth. The inset graph of

Fig 4.5(b) shows that as the depth of modulation is increased, the deviation from a Gaussian shape increases. For bandwidth values less than 550 MHz it can be seen that χ^2-values are less than 0.1 such that the experimental spectra closely resemble a Gaussian shape. The amplitude modulation induced distortion of the observed spectral distribution is more pronounced for triangular and inverse hyperbolic tangent waveforms than for sinusoidal modulation (Fig 4.3a, Fig 4.4a and Fig 4.5a). This, in part, may be due to distortion introduced by digital-to-analogue conversion of the arbitrary waveform generator and also the effect of higher harmonics of fundamental modulation frequency in case of the other two modulation functions. We note that the spectral distributions of the amplified diode output (10 W) are found to be the same as before amplification, irrespective of what particular modulation function is used for spectral shaping.

4.4 Summary

In summary, we have presented the first diode-oscillator fiber-amplifier (MOPA) system that offers spectral shaping and high output power around 1080 nm. The diode laser is a three-section DBR diode, with DC bias at the gain section. In addition, the phase section is driven independently with an RF arbitrary waveform superimposed on a DC current to shape and broaden the narrow band laser bandwidth to greater than 1 GHz. The effect of modulation by different RF waveforms on the diode spectrum was investigated in three examples, and it was found that the spectral distribution could be controlled via the RF waveform. The diode power of 40 mW was amplified in an Yb-doped fiber, which retains the oscillator spectral characteristics at 10-Watt-level powers, and with high suppression (50 dB) of ASE spectral background.

The combined advantages of the spectral shaping available via the diode laser and the high power obtained by the fiber amplifier results in a source

well suited for optical pumping of Doppler-broadened gases with high efficiency. This MOPA system when utilized in an optical pumping experiment should yield large volumes of gases with high polarization of the nuclear spins.

Chapter 5

Fiber amplification of picosecond-pulses from a widely-tunable mode-locked diode laser[1]

In the previous chapters, the ease with which diode lasers can be modulated via their injection current was used at frequencies in the MHz range to achieve simple spectral broadening and more sophisticated spectral shaping. However, depending on the particular device, diode lasers can be modulated at much higher frequencies, in the GHz range. This property can be used to achieve active mode-locking allowing the simple generation of ultrashort pulses with high repetition rates. The suitability of Ytterbium-doped fibers for the amplification of diode lasers operating in the region of 1.06μm, also shown in the previous chapters, can then be exploited to amplify such pulse trains to high average powers. This chapter describes the first realization of the fiber amplification of a widely tunable actively mode-

[1]Published as: B.Adhimoolam et al., IEEE. Photon. Technol. Lett.,**18**, 838- 840, 2006

locked diode laser at a wavelength around 1.06μm in an Ytterbium-doped fiber [96]. The actively mode-locked diode laser produces picosecond pulses at GHz repetition rate across its tuning range, whose power is amplified to multi-Watt level in a 36m long Ytterbium-doped fiber amplifier. This chapter is organized as follows. Section 5.1 introduces the need for near-IR picosecond pulses with high peak powers, and the advantage of fiber amplifying a tunable, actively mode-locked diode laser in realizing this will be discussed. The experimental setup consisting of the external-cavity diode laser in Littrow configuration and an Ytterbium-doped fiber amplifier will be presented in the section 5.2. This is followed by a detailed characterization, where experimental results such as the pulse duration, wavelength tuning and the output power measurements are presented in the section 5.3. Finally we conclude the chapter by a brief summary.

5.1 Introduction

Tunable optical sources with a picosecond pulse duration operating in the near-IR regime are of interest for a wide range of applications. For many spectroscopic methods, picosecond sources offer a good compromise between spectral and temporal resolution, while the high peak powers achievable allow efficient excitation of non-linear optical processes such as coherent anti-stokes Raman scattering (CARS) [97]. Moreover, tunable near-IR picosecond sources with high peak power are also highly suitable for CARS microscopic imaging for the following reasons. First, the use of near-IR sources significantly reduces the non-resonant background from the resonant signal in CARS imaging experiments and effect of the Rayleigh scattering in the sample is minimized, hence the near-IR sources penetrate deeper into the sample [98]. Second, the picosecond pulses provide better signal-to-background ratio because their linewidths are of the order of the typical Raman bandwidths. Thus, the use of tunable picosecond sources provide high contrast CARS images [99]. High peak powers also enable effi-

cient nonlinear frequency conversion via, for example, an optical parametric oscillator (OPO) while the moderate pulse duration permits the use of long non-linear crystals, further enhancing the efficiency of the OPO. The combination of a near-infrared picosecond laser with a synchronously-pumped singly-resonant OPO results in a particularly flexible tunable picosecond source [100, 101]. Tuning of the pump laser allows wide-range tuning of the OPO signal and idler wavelengths [35, 102], while rapid tuning of the idler wavelength can be achieved by varying the repetition rate of the pump laser [103]. Mode-locked external-cavity diode lasers [104, 105] meet many of the requirements for such a pump laser. The external diffraction grating provides a simple means of wide wavelength tuning while a short external cavity results in high repetition rates (of the order of GHz). These lasers when used to synchronously pump OPOs, allow compact OPO cavities. Mode-locking can be simply achieved by current modulation, allowing a variable repetition rate for rapid OPO tuning [103]. However, the low output powers from mode-locked diode lasers generally require further amplification before they are sufficient to pump an OPO. This has previously been demonstrated using semiconductor amplifiers [100, 103], although the powers achieved remained moderate. Ytterbium-doped fiber amplifiers are well suited for the amplification of short pulses in the 1–1.1 μm region [106, 107, 108] and appear to offer an ideal amplification medium for mode-locked diode lasers operating at these wavelengths. Such a system would then translate the described benefits of mode-locked diode lasers to high average powers while offering reduced complexity compared to devices based on mode-locked fiber oscillators. Surprisingly, therefore, mode-locked diode lasers and diode-laser-fiber-amplifier systems operating in the 1–1.1 μm range do not appear to have been widely investigated. Reported results are restricted to a mode-locked diode laser delivering 1 ps pulses with 13 mW average power [109], and a gain-switched injection-seeded system with subsequent fiber amplification operating at a fixed wavelength [110]. In this chapter, the first demonstration of a mode-locked and widely tunable

diode-oscillator fiber-amplifier system operating in the region of 1.06 μm is presented.

5.2 Experimental setup

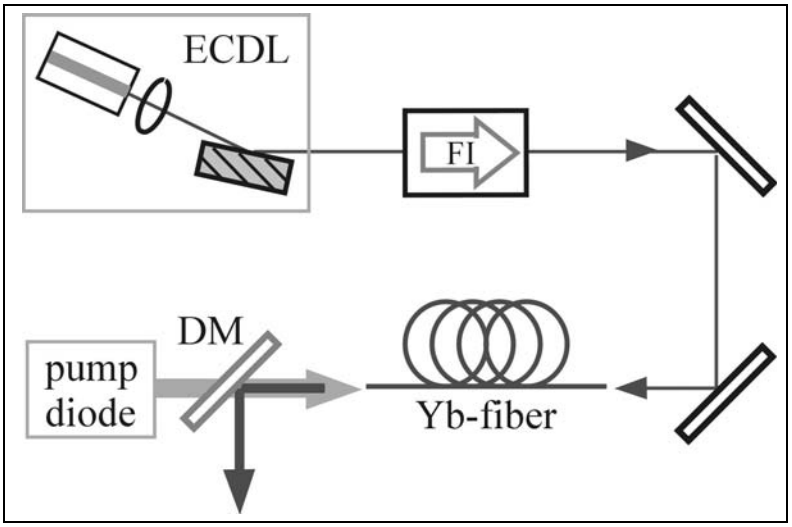

Figure 5.1: Setup of the pulsed diode-oscillator fiber-amplifier system. ECDL: external cavity diode laser in Littrow configuration, FI: 60-dB Faraday isolator, Yb-fiber: Ytterbium-doped fiber amplifier, DM: dichroic mirror, pump diode: 25-W fiber-coupled 976-nm diode bar.

The experimental setup is shown schematically in Fig 5.1. The diode laser is a single-stripe InGaAs-GaAs diode, with an anti-reflection coated output facet specified to a residual reflectivity of less than 10^{-5}. The output of the diode laser is collimated using a lens (C220 TM-B, f=11mm AR coated for wavelengths 600nm-1100nm). The diode laser is mounted in an external cavity, where feedback is provided by a grating (1200 lines/mm) in Littrow-configuration, i.e., where about 15% of the diode laser power is coupled back into the diode laser via the 1st diffraction order, while a larger portion (40%) of the diode laser emission is coupled out via the

$zero^{th}$ diffraction order [111]. The diode is connected via a bias-T to a DC biasing supply and a radio-frequency (RF) driver (Anritsu 69147A synthesizer and 30-dB amplifier). To allow an efficient modulation of the driving current in the GHz-range, the diode is equipped with an impedance matching circuit, which showed a maximum impedance match (minimal reflection of AC power) between the diode laser and the RF source at a frequency of 1.4GHz. After transmission through a 60 dB optical isolator, the diode laser output is coupled into the Ytterbium-doped fiber core of the 36-m long double-clad large mode area (LMA) fiber[1] for amplification. The details of the fiber amplifier setup can be found in chapter 3. An optical spectrum analyzer (OSA) with 0.015 nm (4 GHz at 1060 nm) resolution (ANDO type AQ6317) and a home-built interferometric auto-correlator was used to measure the diode laser wavelength and the pulse duration before and after amplification. The output power measurements were performed with a calibrated power meter (Newport thermopile 1815C).

5.3 Results - pulse duration and output power

By changing the angle of the feedback-grating of the external cavity, the wavelength of the diode laser can be set to any wavelength in the range from 1010 to 1085 nm with a side mode suppression of better than 35 dB. For mode locking of the diode laser we use an RF drive frequency of 1.4 GHz and a cavity length of 107 mm. At a DC current of 75 mA and an RF power of 30 dBm, the diode laser generates about 15 mW of average output power across the entire tuning range.

The average power obtained after fiber-amplification with up to 25 W pump power is shown in Fig 5.2 vs. the diode laser wavelength. As can be seen, the power is well above 9 W in a wide wavelength range from 1055 to 1085 nm. The flat shape of the output power vs. wavelength indicates that the fiber gain is well saturated, such that the output power scales with the

[1]Manufactured by IPHT Jena, Germany

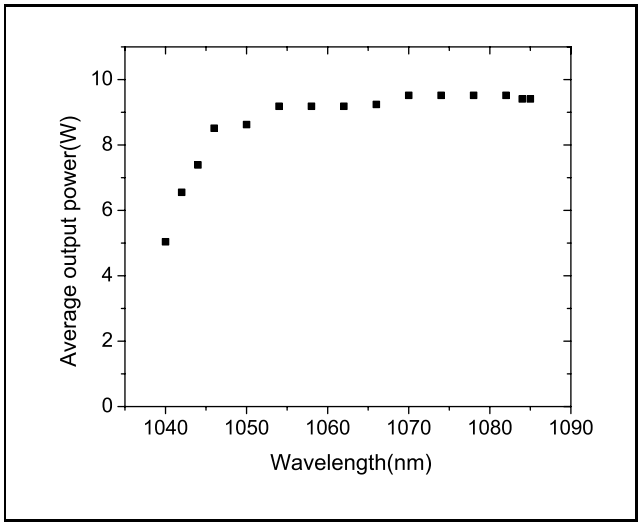

Figure 5.2: Average output power obtained after fiber-amplification of the pulses as a function of diode laser wavelength.

available pump power. At the lower end of the tuning range (below 1050 nm), a drop in the output power can be seen. Here, the diode wavelength falls in the edge of the Ytterbium gain bandwidth. Correspondingly, operation below this value leaves unsaturated gain in the fiber, which can lead to unwanted self-pulsing of the amplifier at central (higher gain) wavelengths as described in chapter 2. Such self-pulsing was prevented by gradually reducing the pump power to 19 W when tuning toward 1040 nm.
Fig 5.3 shows interferometric autocorrelation traces of the diode laser pulses before amplification (upper graph, solid black) and after amplification (lower graph). The dashed black curves are a best fit of the autocorrelation envelopes, with the pulse duration T and a linear chirp as fit parameters, and assuming a Gaussian temporal pulse shape of the light field,

$$E(t) \propto exp\{\frac{-1+iC}{(t/T)^2}\}, \tag{5.1}$$

with C being the chirp parameter [112]. The fit yields pulse durations about 37 ps and 30 ps, and a chirp parameter of 2.4 and 1.4, before and

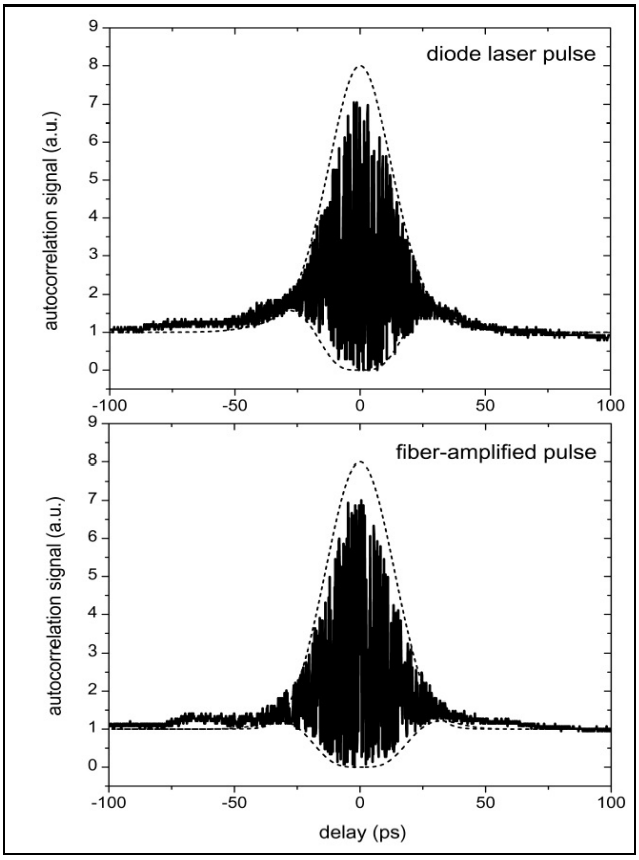

Figure 5.3: Autocorrelation of the diode laser pulses before (upper graph) and after amplification (lower graph) in the Ytterbium-doped fiber, with the wavelength set to 1058 nm. Both graphs show the respective interferometric autocorrelation (solid black curves) and the envelope (dashed black curves).

after amplification, respectively. Such pulse durations and chirp are commonly observed in pulses from diode lasers [105]. Within the tuning range, the pulse duration varies between 28 and 44 ps before, and between 20 and 33 ps after amplification. The reduced pulse duration after amplification could possibly be due to the non-uniform amplification of the pulse, which

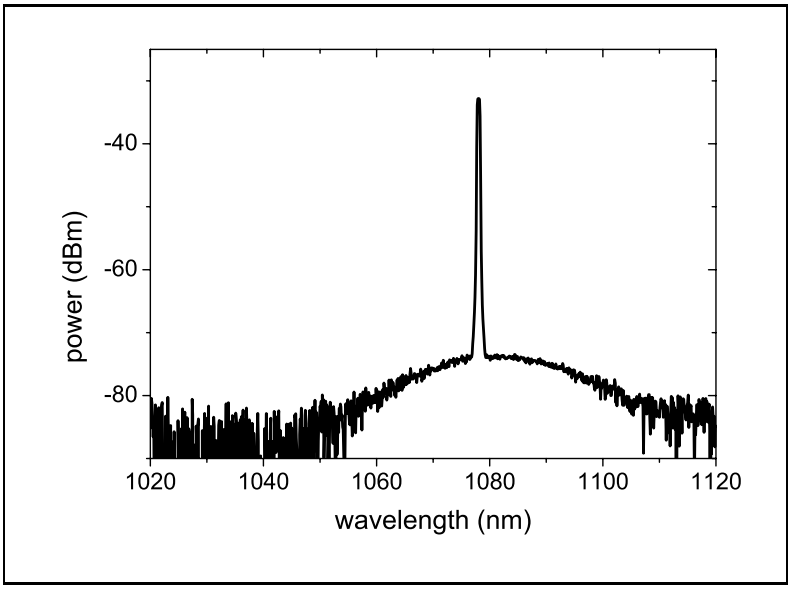

Figure 5.4: Spectrum of the fiber amplifier emission at an average output power of 2 W, when seeded with 35-ps pulses at a wavelength of 1078 nm. The background is suppressed by more than 40 dB with respect to the maximum emission at the seed wavelength.

can be explained as follows: The energy stored in the fiber obtained by inversion of the Ytterbium ions via continuous pumping provides high gain, and when the pulse arrives, the front end of the pulse depletes the high gain in the fiber and hence experiences higher amplification compared to the later part of the pulse, which experiences a lower gain. This can lead to reduction of pulse duration of the amplified output. The non-uniform amplification could also be the reason for the reduction in the chirp factor of the amplified pulses.

The time-bandwidth product of the pulses was determined, before and after amplification, by using the OSA. We measured a constant spectral bandwidth of 0.18 nm (50 GHz) within the spectral resolution, before and after amplification, and obtain a time-bandwidth product of 1.8 and 1.4, re-

spectively. These values are about a factor of 3 to 4 higher than the Fourier limit for a Gaussian pulse shape, but the pulse duration can possibly be reduced with suitable dispersion compensation [113]. Finally we measured the spectral purity of the diode-fiber system with regard to background from amplified spontaneous emission (ASE), with the OSA resolution set to 0.5 nm.
Fig 5.4 shows a spectrum of the output over a wide range, from 1020 to 1120 nm, thus covering the entire gain bandwidth of the fiber, when the diode oscillator was set to a wavelength of 1078 nm. It can be seen that the ASE background is rather weak and lies typically 40 to 50 dB below the emission at 1078 nm. When spectrally integrating the ASE we find that more than 99% of the 9 Watt output from the diode-fiber system is emitted at the wavelength of the diode oscillator. With these properties, the system should allow for an efficient wavelength conversion in synchronously pumped singly-resonant OPOs, due to their low average threshold of typically a few hundred mW. Due to the moderate pulse duration of the laser system presented (e.g., as compared with fs pump sources), a relatively narrow bandwidth of 50 GHz offers spectroscopic resolution in the mid-IR. In the near-IR region, the high peak power picosecond pulses combined with the wide tuning range would suggest the possibility of applying the fiber-amplified output directly in applications such as CARS microscopy.

5.4 Summary

In this chapter, the first realization of the fiber amplification of picosecond pulses with GHz repetition rate produced from an actively mode-locked diode laser, with wide tuning around 1.06μm has been presented. The diode laser is mounted in external cavity with a grating providing the wavelength selection in Littrow configuration. The wavelength tuning around 1.06μm allowed the diode output to be amplified in an Ytterbium-doped

fiber amplifier when operated in a master oscillator-power amplifier setup. The broad gain bandwidth of the Ytterbium-doped fiber ensures amplification over most of the tuning range. By this, an average power of 15 mW from the diode oscillator with wavelength tunability extending over 45 nm and providing pulse durations around 30 ps at a repetition rate of 1.4 GHz is amplified to a maximum average power of 9.5 W. The output power of 9.5W is well above the threshold of typical ps-pulsed, synchronously-pumped SROs (generally a few hundred mW) [100]. The combined advantages of the mode-locked diode laser with the fiber amplifier result in a source well suited to synchronous pumping of a singly-resonant OPO. The wide grating-tuned coverage of 45nm in the 1.06μm region would translate to approximately over 700nm in the mid-IR - calculated from SNLO for a 30μm poling period of PPLN [33], while the possibility of varying the repetition rate electronically holds potential for rapid tuning of an OPO over smaller ranges [102, 103]. The high repetition rate of 1.4GHz would correspond to an OPO cavity (ring) round-trip length of only around 214mm in synchronous-pumped operation, allowing compact devices to be used.

Chapter 6

Widely and rapidly tunable semiconductor master-oscillator fiber-amplifier around 1080nm[1]

For realizing mid-infrared detection of trace gas molecules in real-time via a singly resonant optical parametric oscillator (SRO), in chapter 2, we had summed up our requirements for the SRO pump source as follows: 1) operation at wavelength around 1.08μm, with 2) the ability to provide large continuous near-IR tuning and 3) a multi-Watt-level output power to surpass the threshold pump power of the SRO. Further, 4) narrow-linewidth, less than the pressure broadened linewidth $\approx$ 0.5GHz of mid-IR spectral lines and 5) a rapid tuning of the pump source is desired, achieved by electronic means. Rapid tuning over wide wavelength ranges in principle

[1]Published as: B.Adhimoolam et al., submitted for publication in IEEE. Photon. Technol. Lett., 2006

can be easily achieved, by using a broad-band laser source with a widely and rapidly tunable band-pass filter [114, 115]. In this chapter, we report on a laser source operated in a master-oscillator power-amplifier (MOPA) setup, which simultaneously satisfied all the above requirements. The novel master-oscillator consists of a semiconductor amplifier based laser, which is widely and rapidly tunable around a wavelength of 1.08μm, and an Ytterbium-doped fiber as the power-amplifier [116]. The combination of the two results in a source with rapid tuning over tens of nano-meters at multi-Watt power levels. This chapter is organized as follows. Section 6.1 discusses the need for rapidly tunable near-IR lasers with Watt-level powers and describes the advantages of fiber amplification of a widely tunable diode laser in realizing such a source. The experimental setup consisting of the semiconductor amplifier based laser and an Ytterbium-doped fiber amplifier used to amplify the laser output will be presented in the section 6.2. This is followed by the detailed characterization of the laser, where the experimental results such as the wide and rapid wavelength tuning and the output power measurements are presented in the section 6.3. Finally we conclude the chapter by a brief summary, where we suggest alternative methods, to achieve rapid and wide wavelength tuning in the near-IR region.

6.1 Introduction-Need for rapidly tunable lasers

Near-infrared lasers with wide wavelength tuning and a fast tuning rate, so-called swept wavelength lasers, are of importance for many applications such as Fourier domain optical coherence tomography, optical frequency domain reflectometry and fiber grating array monitors [117, 118, 119]. Making such spectral properties also available in the mid infrared would enable a wide range of spectroscopic sensing applications, e.g., when a large variety of molecules must be distinguished in a short time. In addition, if the source is to be used for mid-infrared spectroscopy of gases, the spec-

tral width should at least be narrower than the typical widths of spectral features encountered (of the order of 0.5 GHz at atmospheric pressure). High-power (Watt-level) mid-infrared radiation can be generated via optical parametric oscillators (OPOs), in particular, continuous wave, singly resonant OPOs (cw-SROs) have been shown to be well suited for molecular spectroscopy. However, the relatively high pump power at threshold requires typically 5 to 10W of pump radiation for efficient operation of the SRO. As was discussed in chapter 2, an important property of an SRO is that it transfers the spectral characteristics of its near-IR pump laser (tuning rate, tuning range, linewidth etc.) to the mid-IR. Thus the development of pump lasers with appropriate spectral properties is of great importance and is the central theme of this thesis. A number of specific properties are desirable. A wide tuning range allows many different spectroscopic targets to be addressed. Rapid tuning (which, in practice, implies some electronic tuning mechanism) allows spectra to be acquired and monitored in real time. Finally, a sufficiently narrow linewidth is required to allow specific spectral targets to be unambiguously addressed. We have seen that a fiber laser or MOPA concept is an attractive route to achieve such performance. However, achieving all these requirements simultaneously remains problematic. Wide and rapid pump tuning of an OPO have been demonstrated using a fiber laser tuned by an acousto-optic tunable filter (AOTF) [15]. However, the poor spectral selectivity of the AOTF resulted in a linewidth of 30 to 100 GHz, which would not provide sufficient resolution for most applications involving spectroscopy of gases under ambient pressure. Conversely, a fiber MOPA system seeded with a DBR laser of the type described in chapters 3 and 4 has been used to achieve high-resolution pump tuning of an OPO [34]. In this case, however, the limited total tuning range of the DBR laser (approximately 2nm) required other tuning mechanisms (e.g. temperature or grating period) to be applied to the OPO if wide-range mid-IR tuning was to be achieved. Thus rapid, wide-range, spectral profiling was not possible.

In this chapter, we describe a novel near-infrared diode-fiber MOPA system that provides up to 9 Watts output power in the range from 1060 to 1100nm, enables rapid tuning in that range, and provides a sub-GHz spectral linewidth.

6.2 Experimental setup

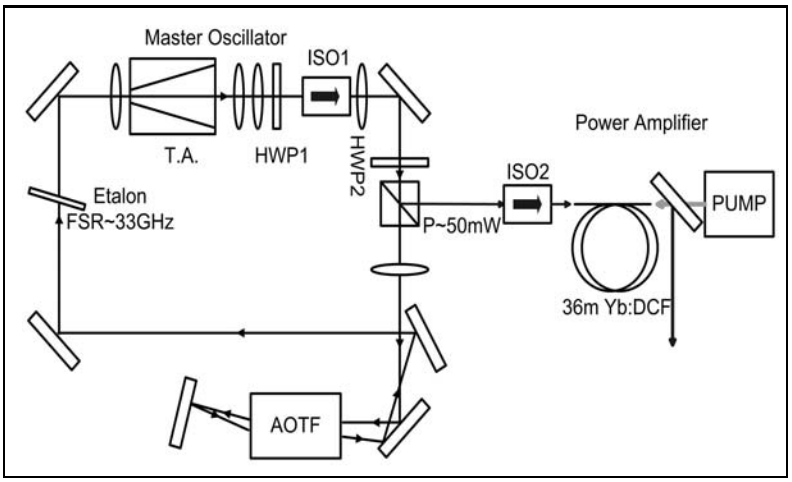

Figure 6.1: Experimental setup: T.A: tapered semiconductor amplifier, HWP:half-wave-plate; ISO: 60dB Faraday isolator; AOTF: acousto-optic tunable filter; PBS: polarizing beam-splitter; Yb DCF: Ytterbium doped double-clad fiber; DM: dichroic mirror; PUMP: 25W diode laser.

The master-oscillator, as shown in Fig 6.1, is based on a tapered GaAs semiconductor amplifier (aperture dimensions: input $\approx 3\mu$m; output $\approx 190\mu$m; and length ≈ 2.75mm) with a specified gain bandwidth of 50nm centered at 1.08mm[1]. The output of the tapered amplifier is collimated by a C230-TM-C lens (f=4.5mm, N.A=0.55) and circularized by a cylindrical lens (f=50mm). The amplifier is placed in a 140cm long ring cavity where

[1]Manufactured by Eagleyard Photonics GmbH, Berlin, Germany

unidirectional operation is ensured by a 60dB Faraday isolator. Variable output coupling is enabled by the combination of a polarizing beam-splitter and a half-wave-plate. An intra-cavity AOTF (Brimrose-TEAF7-0.8-1.4-H, Tuning range: 800-1400nm) used in a double-pass configuration provides rapid electronically-controlled wavelength selection. A solid-state etalon (free spectral range, FSR=33GHz, R=80%) in the cavity acts as a narrowband filter. A scanning confocal Fabry-Perot interferometer with 3GHz FSR and Finesse $\approx$ 100 was used to measure the laser bandwidth when the output wavelength is fixed. Absolute wavelength measurement was obtained from an optical spectrum analyzer (OSA) with a resolution of 0.015nm (Ando AQ-6317). A low-Finesse etalon with a FSR of 200 GHz, followed by a photodiode, was used as a real-time wavelength monitor during tuning. Following 60dB isolation and polarization control, the laser output is used to seed a double-clad large mode area (LMA) Yb-doped fiber, 36m in length. The details of the fiber amplifier can be found in chapter 3.

6.3 Results-Wavelength Tuning and output power

Without the intra-cavity etalon and with a fixed AOTF drive frequency, the spectral bandwidth of the laser varies between 30GHz and 100GHz, depending on the AOTF drive frequency. Inserting the solid etalon into the cavity reduced the linewidth to below 650MHz, as measured with the scanning interferometer. Rapid and wide tuning between 1061nm and 1097nm is accomplished by sweeping the AOTF driver frequency between 88MHz and 92MHz. In this mode of operation, the laser tunes by hopping from one resonant mode of the intracavity etalon to the next, as the wavelength coarsely selected by the AOTF is swept. The modes of oscillation (transiently) assumed during AOTF sweeping can be fine tuned by rotating the intra-cavity etalon.

Fig 6.2(a) shows the spectrum of the laser for a fixed AOTF frequency and

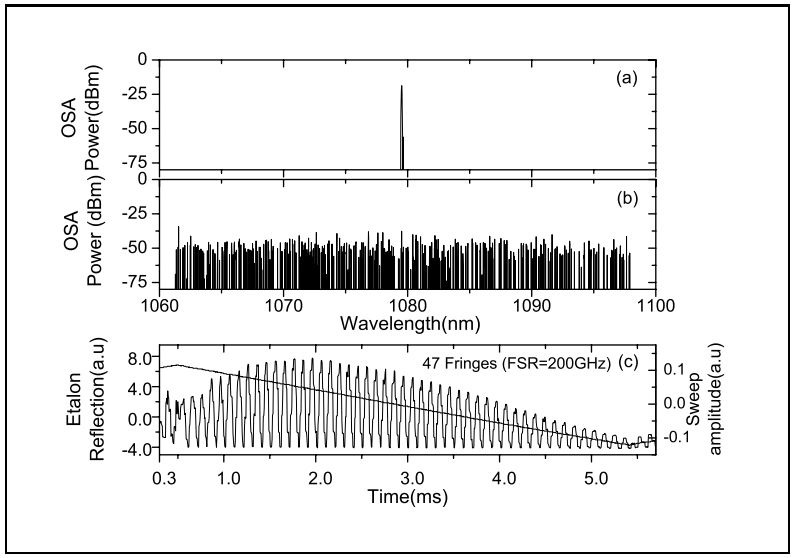

Figure 6.2: The laser oscillator's output spectrum. Subfigure (a) is the spectrum as measured by an OSA when the AOTF frequency is held fixed. Subfigures (b) and (c) shows the time-averaged spectrum and the simultaneously recorded fringe pattern from the 200 GHz monitor etalon as the laser wavelength is swept over 36 nm at a rate of 100 Hz.

etalon angle as measured with the OSA. Fig 6.2(b) shows the time-averaged spectrum when the laser wavelength is periodically swept. The wavelength sweep was accomplished by applying a 100 Hz, triangular voltage to the AOTF driver, which causes it to linearly sweep the drive frequency and yields a measured laser wavelength coverage of 36nm as seen in Fig 6.2b. While this measurement demonstrates the spectral coverage achieved, the number and spacing of the data points stored by the OSA, coupled with the mode-hopped tuning mechanism, does not allow reliable interpretation of the spectrum on a fine scale. In order to investigate whether the laser tuning is monotonic, the output was monitored with the 200GHz FSR etalon. Fig 6.2(c) shows a monitor trace as the laser wavelength is increased by 36nm, which corresponds to 47 fringes of the monitor etalon. The smooth

and periodic variation of the fringe pattern shows that the tuning is indeed monotonic.

To reveal further details, Fig 6.3 (a) and (b) show the magnified OSA

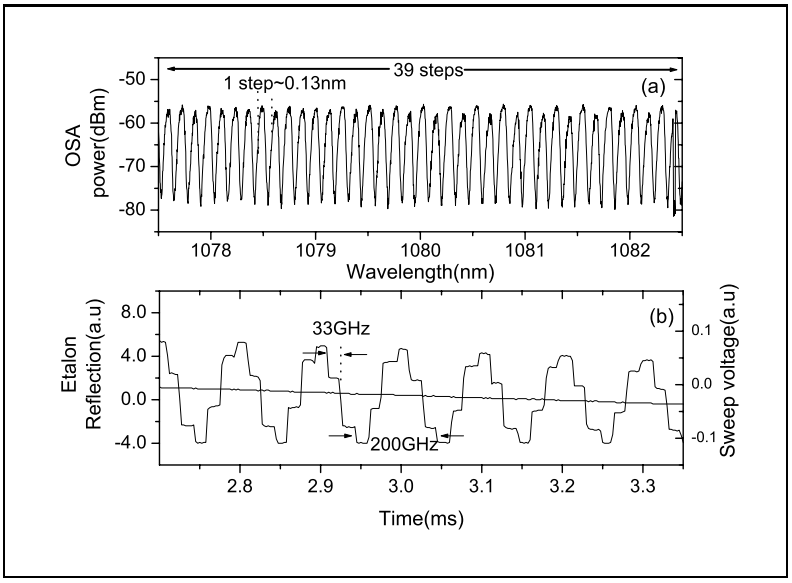

Figure 6.3: Tuning over 5 nm in steps of 33GHz, corresponding to the FSR of the intra-cavity etalon (a) Averaged output spectrum, observed at the spectrum analyzer. (b) Monitored at the 200GHz FSR etalon.

spectrum and monitor etalon fringe pattern over a smaller, 5 nm, range of Fig 6.2 (b) and (c). It can be seen in Fig 6.3 (a) that, on average, the laser tunes in steps of 0.13nm, which corresponds to the 33GHz FSR of the intra-cavity etalon. This is also confirmed by the observation that there are six such steps in every 200 GHz FSR of the monitor etalon (Fig 6.3(b)). Fig 6.3(b) also verifies that these steps occur sequentially and systematically within a single sweep. It should be noted that we observed such systematic tuning only for sweeps of increasing wavelength, while sweeps of decreasing wavelength showed irregular fringes with the monitor etalon. The reason for this hysteresis-type of tuning asymmetry is currently not

well understood, but it may involve the spectrally asymmetric gain profile (see Fig 6.2c) and corresponding build-up and decay times of modes in relation to the time the AOTF requires to tune to the next intracavity-etalon frequency.

Small angular adjustments of the intra-cavity etalon enables fine wave-

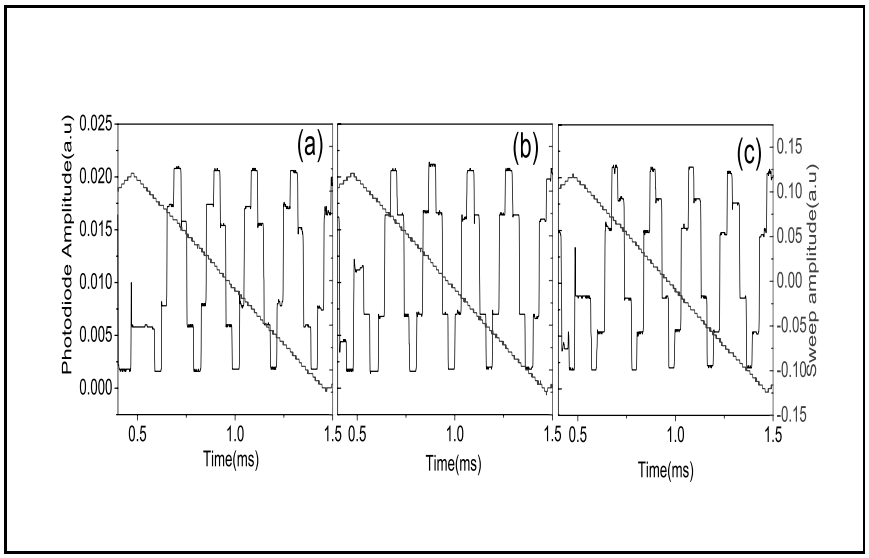

Figure 6.4: Tuning over 3 nm, monitored at 200GHz FSR etalon. Subfigures (a)-(c) shows the variation in the step positions for different intracavity etalon angles, indicating that the etalon angle provides fine control over the wavelengths the frequency sweep accesses.

length tuning. More accurately, adjusting the etalon angle systematically changes the wavelengths along which the laser step-tunes. Fig 6.4(a)-(c) shows the effect of finely adjusting the angle of the intracavity etalon, when the laser is tuned over 3nm. It can be seen that the position of the steps, corresponding to the intra-cavity etalon cavity modes are shifted with respect to each other as the angle of the etalon is adjusted. In this way, the entire spectrum over the gain bandwidth of the laser can be accessed.
The average output of the laser while tuning over the 36nm was 50mW. The

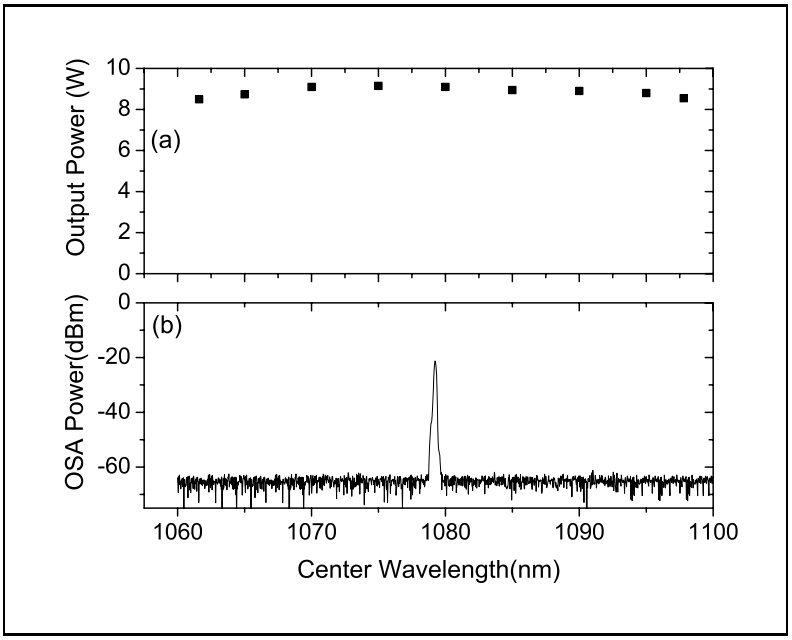

Figure 6.5: The amplified output when the oscillator is tuned over 36nm. Subfigure (a) shows the amplifier output power variation with seed wavelength. Subfigure (b) shows the time averaged amplifier output spectrum as measured by an OSA.

seed power available in front of the fiber amplifier was slightly less (35mW), which is due to the optical isolator and polarization optics. The output power of the amplifier was measured using a calibrated Silicon photodiode. As shown in Fig 6.5(a), the amplifier output power varies between 8.5W and 9.1W over the tuning range. This can be explained by the oscillator providing an output power which is high enough to saturate the amplifier within most of the tuning range, but which is insufficient to saturate the amplifier at the edges of the tuning range. Finally, of concern for MOPA systems is the amount of spectrally broadband background emission that can be generated by amplified spontaneous emission (ASE) from the diode oscillator or the fiber amplifier. Fig 6.5(b) shows the output spectrum from

the MOPA system when the oscillator wavelength is fixed at 1079nm and the amplified power is 9W. The spectrum shows that ASE is suppressed by more than 40dB. Similarly, the suppression over the entire tuning range was found to be between 30-40dB which implies negligible losses due to ASE and that the 9W of measured output power is concentrated within the spectral bandwidth of the seed laser.

6.4 Summary

In summary, we have described the properties of a MOPA system comprising a master oscillator based on a semiconductor tapered amplifier and an Ytterbium-doped fiber based power amplifier. The system is capable of being systematically tuned over a wide wavelength range at stable multi-Watt powers. The 50mW laser output with a wide tuning range of 36nm, swept at a rate of 100Hz was amplified to over 9W. The output powers obtained, the wide spectral coverage in combination with sub-GHz spectral bandwidth and high tuning rates are of interest for pump-tuning a singly-resonant optical parametric oscillator to efficiently down-convert such spectro-temporal properties to the mid infrared spectral region.
Although, tunable filters such as AOTF provide wide and rapid tuning when used as an intra-cavity element with broad-band laser sources, the band-pass of an AOTF is of the order of 30-100GHz. This is rather broad-band for spectroscopic detection of typical gases at ambient pressures. Thus, it was required to introduce an additional frequency-selective element, in the form of an etalon, into the cavity. By this means, the instantaneous linewidth of the laser was reduced to 650MHz. An obvious consequence of this is that the laser now tunes in steps, corresponding to the etalon free spectral range of 33GHz. Small angular adjustments of the etalon enabled the position of these steps to be varied systematically, thus allowing access to the intermediate wavelengths. It may be thought that the use of an etalon in this way negates the rapid tuning advantage of the AOTF. How-

ever, the systematic manner in which the tuning steps can be controlled by small changes in etalon angle suggest a novel approach to achieving rapid and wide spectral coverage with high resolution.

Conventionally, a tunable laser combining an etalon with a less selective tuning element, such as the AOTF, would be tuned by varying the angle of the etalon and synchronously tuning the AOTF to track a single etalon mode over many etalon free spectral ranges. In that case, the overall tuning rate is limited to that determined by the mechanically tuned etalon. Additionally, the tuning range is limited by the etalon losses which increase rapidly at large angles. The systematic step-wise tuning observed here suggests that a sampled tuning approach could be adopted. In this case, data could be recorded at each tuning step within a single AOTF sweep and the position of these steps could then be shifted in a controlled manner for subsequent AOTF sweeps. By interleaving a number of these sampled spectra, full spectral coverage could be reconstructed. By this means, much of the rapid tuning advantage of the AOTF is retained while the total etalon tuning range is limited to one free spectral range, thus limiting the required angular variation and associated losses as well as the required speed in tilting. In the limiting case, the position of the tuning steps would be shifted by the laser linewidth between each AOTF sweep and the full tuning range could be addressed, at the resolution defined by the laser linewidth, in a total number of AOTF sweeps corresponding to the ratio of the etalon FSR to the linewidth. In the case of the laser described here, this would imply a total of 50 AOTF sweeps resulting in the full 36nm tuning range being covered with 650MHz resolution in 0.5 seconds.

Chapter 7

Summary and Conclusions

In this thesis, the investigation of a class of near-IR laser sources comprising diode-laser-based master oscillators combined with Ytterbium-doped fiber amplifiers has been described. The combination of the flexible modulation and tuning characteristics of the diode-based master oscillators with the high power capabilities of the fiber amplifier allow a variety of high-power spectro-temporal operating regimes to be explored based on a common device concept. In addition the limitations, due to nonlinear effects, on the fiber amplification of such diode-laser master-oscillators have been investigated and practical strategies for achieving stable amplifier operation identified. The results presented show that diode lasers when operated in combination with a fiber amplifier, provide a particularly flexible route to rapid, wide-range tuning and mode-locked operation with Watt-level powers in the near-infrared region. The primary motivation for this work has been to develop laser systems suitable for pumping singly-resonant optical parametric oscillators (SROs) for spectroscopic applications in the mid-infrared. SROs have been shown to effectively transfer the spectral properties of their near-infrared pump source to the mid-IR [34]. Thus, the development of sources such as those described here, offering a variety of novel spectral and temporal modes of operation combined with the Watt-level powers required

to pump an SRO, provide a route to achieving, for example, rapidly-tuned or picosecond-pulsed operation in the mid-IR. Additionally, the sources described in this thesis have potential for direct utilization in applications such as OCT [117], CARS [97] and He pumping [90].
To summarize, we have investigated the fiber amplification of three diode based laser sources.

1. A distributed Bragg reflector (DBR) diode laser at a wavelength around 1080nm,

2. an actively mode-locked diode laser (InGaAs-GaAs) widely tunable around 1060nm,

3. and a semiconductor amplifier based laser, with an intra-cavity AOTF providing wide and rapid tuning around 1080nm.

The properties of the above mentioned laser sources and the results obtained after amplification are summarized below.

DBR diode laser in combination with Ytterbium doped fiber amplifier

The DBR diode laser was operated in combination with a Ytterbium-doped fiber amplifier in a master-oscillator power-amplifier system. The DBR diode laser was a three-section device, which emits at a wavelength around 1080nm and had a narrow spectral bandwidth of 30MHz. The DBR diode laser output was amplified in two Ytterbium-doped fiber amplifiers of length of 36m and 50m. The undesired self-pulsing common in fiber amplifiers was suppressed by a weak modulation of the diode laser injection current. Self-pulsing effects were systematically studied in both the amplifiers as a function of DBR diode laser parameters such as seeding power and the bandwidth. A maximum stable output of 10W and 12W were produced from the 36m and 50m fiber, respectively. The 36m long fiber was chosen ahead of the 50m long fiber for our power amplification purposes, as the

maximum stable output produced was higher for a given narrow bandwidth of the laser. The amplified output obtained is sufficient to operate an SRO and produce mid-IR radiation of sufficiently narrow bandwidth to resolve mid-IR spectral lines.
In addition to suppressing self-pulsing, these DBR diode lasers were subjected to much stronger modulation, this resulted in a much broader bandwidth in the GHz range. The multi-section construction of the diode laser was utilized to apply a DC bias to one section and frequency modulate the other section. Here, we DC biased the gain section and modulated the phase section using different waveforms to generate broadened spectra of arbitrary shape. Of particular interest was the Gaussian shape, which was obtained by modulating the diode laser by an arctanh waveform. Such sources at Watt-level power have potential application in optical pumping of Doppler broadened transitions.

Mode-locked diode laser in combination with Yb-doped fiber amplifier

Here, the MOPA system consists of an actively mode-locked diode laser as the master-oscillator and an Ytterbium-doped fiber amplifier as the power-amplifier. The actively mode-locked external cavity diode laser could be tuned from 1010nm to 1085nm. The broad gain bandwidth of the Ytterbium-doped fiber ensures amplification over 45nm of the above tuning range from 1040 to 1085nm. Thus, an average power of 15 mW from the diode oscillator output extending over 45 nm tuning range and providing pulse durations around 30 ps at a repetition rate of 1.4 GHz is amplified to an average power exceeding 9W over most of the tuning range. The output power is well above the threshold of typical synchronously-pumped ps SROs. As a pump source for a synchronously-pumped singly-resonant OPO, this system offers the possibility of wide-range mid-IR tuning and rapid tuning via variation of the repetition rate [103]. In addition, the

high repetition rate would allow compact OPO cavities to be used.

Rapidly tunable diode laser in combination with Yb-doped fiber amplifier

The MOPA system used here, comprises of a master-oscillator based on a semiconductor tapered amplifier and an Ytterbium-doped fiber based power-amplifier. The semiconductor amplifier has a broad gain bandwidth of around 50nm. The semiconductor amplifier is placed in a unidirectional cavity, that includes acousto-optic tunable filter (AOTF), which provides wide and rapid wavelength tuning. Narrow-bandwidth (sub GHz) operation of the laser of the laser was achieved by the introduction of a solid-state etalon in the cavity. The 50mW laser output with a wide tuning range of 36nm, swept at a rate of 100Hz was amplified to over 9W. The output powers obtained, the wide spectral coverage in combination with sub-GHz spectral bandwidth and high tuning rates are of interest for pump-tuning a singly-resonant optical parametric oscillator to efficiently down-convert such spectro-temporal properties to the mid infrared spectral region.

Conclusions and future work

In conclusion, the results presented in this thesis have shown that MOPA systems based on diode lasers in combination with a fiber amplifier provide a wide range of possibilities for modulation and frequency control at high powers. The power levels available are sufficient to pump a singly-resonant OPO offering the possibility of transferring these tuning and modulation properties to the mid-IR. This combination of simple, flexible modulation and tuning with high power offers possibilities not available using other near-infrared solid-state sources. The work also highlights a number of limitations of the devices investigated and promising directions for future work:

The results presented here demonstrate the suitability of double-clad, large mode area (LMA) Ytterbium-doped fibers for amplifying diode laser based sources to powers of several Watts. Although nonlinear effects can lead to unwanted instabilities when narrow-band seed sources are used, it was shown that this could be overcome by artificial broadening of the seed laser spectrum through modulation. However, in many situations this may not be desirable and amplification while retaining narrow-band output would be required. This can be achieved through the use of recently demonstrated LMA fibers with larger core diameters and shorter lengths. Although requiring coiling to achieve transverse mode operation, such fibers have successfully amplified extremely narrow-band sources to over 100W. Combined with some of the wide-tuning techniques described here, such an approach could enable both wide, rapid tuning and narrow-band sources to be developed. However, demonstrations to date have used seed lasers with outputs of at least several hundred milliwatts. Further investigation is therefore probably required to achieve amplification of the sub-100mW seed sources described here in such amplifiers.

The diode based oscillator in combination with an AOTF has been shown to provide rapid tuning over tens of nanometers in the near-IR region. However, additional bandwidth narrowing elements such as the intra-cavity etalon are required for spectroscopic applications at ambient pressures. Nevertheless, this is a huge step forward towards realizing rapidly and widely tunable mid-IR radiation. Ideally, a single tuning element having both wide coverage and high spectral selectivity would be used to achieve narrow-band widely-tunable operation. Recently, the development of fiber Fabry-Perot tunable filters (FFPTF) at these wavelengths have made such a tuning element available. While offering a similar tuning range to the AOTF, these devices have an extremely high finesse and therefore narrow bandwidths around tens of MHz. Our recent work has demonstrated the use of such a FFPTF in a diode-based master oscillator similar to that described with the AOTF here [120]. A tuning range of 25nm with a linewidth

of 30MHz was achieved, indicating the suitability of such tuning elements in systems of this type. Although, the low damage threshold of these devices still necessitated a complex split-cavity design further development of this technology holds considerable promise for the future.
Overall, it can be concluded that advantages of such MOPA systems based on diode lasers and fiber amplifiers in the near-IR, its suitability to pump and tune SRO to obtain the same spectral properties in mid-IR tuning, will ensure the further investigation into development of such sources.

Bibliography

[1] M. Mürtz, B. Frech, P. Palm, R. Lotze, and W. Urban. Tunable carbon monoxide overtone laser sideband system for precision spectroscopy from 2.6 to 4.1μm. *Opt. Lett.*, 23:58–60, 1998.

[2] H. Preier, Z. Feit, J. Fuchs, D.Kostyk, W. Jalenak, and J.Sproul. Status of lead salt diode laser development at spectra-physics, in monitoring of gaseous pollutants by tunable diode lasers. *Proc. Int. Symposium, Freiburg, Germany*, 158, 1988.

[3] A. N. Baranov J. C. Nicholas and, Y. Cuminal, Y. Rouillard, and C. Aliber. Tunable diode laser absorption spectroscopy of carbon monoxide around 2.35μm. *Appl. Opt.*, 37:7906–7911, 1998.

[4] R.M. Williams, J. F. Kelly, J.S. Hartman, S. W. Sharpe, F. Capasso C.Gmachl D. L. Sivco J. N. Baillargeon M. S. Taubman, J. L. Hall, and A. Y. Choz. Kilohertz linewidth from frequency-stabilized mid-infrared quantum cascade lasers. *Opt. Lett.*, 24:1844–1846, 1999.

[5] S. Wehe, M. Allen, X. Liu, J. Jeffries, and R. Hanson. Tunable solid-state lasers. *41st Aerospace Sciences Meeting and Exhibit, Reno, Nevada.*, pages AIAA–2003–588, 2003.

[6] P. F. Moulton. Tunable solid-state lasers. *Proc. IEEE.*, 80:348–364, 1992.

[7] R.H. Page, K.I. Schaffers, L.D. Deloach, G.D Wilke, F.D. Patel, J.B. Tassano, S.A. Payne, W. F. Krupke, K.-T. Chen, and A. Burger. Cr2+-doped zinc chalcogenides as efficient, widely-tunable mid-infrared lasers. *IEEE J. Quantum Electron.*, 33:609–619, 1997.

[8] S. Schiller and J. Mlynek. Continuous-wave optical parametric oscillators, materials, devices, applications. *Appl. Phys. B.*, 66:664–764, 1998.

[9] D. Boucher, W. Chen, J. Burie, and P. Peze. A novel cw optical laser-based difference-frequency infrared spectrometer, materials, devices, applications. *Ann. Phys.(Paris).*, 23:247–248, 1998.

[10] P. E Powers, Thomas. E. Kulp, and S. E. Bisson. Continuous tuning of a continuous-wave periodically poled tunable lithium niobate optical parametric oscillator by use of a fan-out grating design. *Opt. Lett.*, 23:159–161, 1998.

[11] G. M. Gibson, M. H. Dunn, and M. J. Padjett. Application of continuously tunable, cw optical parametric oscillator for high resolution spectroscopy. *Opt. Lett.*, 23:40–42, 1998.

[12] M. Van Herpen, S. C. Li, S. E. Bisson, and F. J .M. Harren. Photoacoustic trace gas detection of ethane using a continuously tunable, continuous-wave optical parametric oscillator based on periodically poled lithium niobate. *Appl. Phys. Lett.*, 81:1157–1159, 2002.

[13] M. E. Klein, C. K. Laue, D. H. Lee, K. J. Boller, and R. Wallenstein. Diode-pumped singly resonant continuous-wave optical parametric oscillator with wide continuous tuning of the near-infrared idler wave. *Opt. Lett.*, 25:490–492, 2000.

[14] M. Van Herpen, S. E. Bisson, A. Ngai, and F. J .M. Harren. Combined wide tuning and high power of a continuous-wave, singly-resonant optical parametric oscillator. *Appl. Phys.B.*, 78:281–286, 2004.

[15] M. E. Klein, P. Gross, K. J. Boller, M. Auerbach, P. Wessels, and C. Fallnich. Rapidly tunable continuous-wave optical parametric oscillator by a fiber laser. *Opt. Lett.*, 28:920–922, 2003.

[16] Henderson, Angus, and Ryan Stafford. Low threshold, singly-resonant cw opo pumped by an all-fiber pump source. *Opt. Express*, 14:767 – 772, 2006.

[17] J. A. Giordmaine and Robert C. Miller. Tunable coherent parametric oscillation in linbo$_3$ at optical frequencies. *Phys. Rev. Lett.*, 14:973–976, 1965.

[18] R. L. Byer, M. K. Oshman, J. F. Young, and S. E. Harris. Visible cw parametric oscillator. *Appl. Phys. Lett.*, 13:109–111, 1968.

[19] A. Yariv and P.Yeh. *optical waves in crystals*. 1989.

[20] B. E. A Saleh and M. C. Teich. *Fundamental of photonics*. John Wiley and Sons, Inc., New York, first edition, 1991.

[21] W.R. Bosenberg, A. Drobshoff, Jason I. Alexander, L.E. Myers, W. Tulloch, and R.L. Byer. Cw singly-resonant optical parametric oscillator based on periodically poled $LiNbO_3$. *Opt. Lett.*, 21:713–715, 1996.

[22] U. Strossner, J. Peters, Mlynek, Schiller S., J.-P. Meyn, and R. Wallenstein. Single-frequency continuous-wave radiation from 0.77 to 1.73μm generated by a green pumped optical parametric oscillator with a periodically poled $LiTaO_3$. *Opt. Lett.*, 24:1602–1604, 1999.

[23] Robert C. Eckardt, C. D. Nabors, William J. Kozlovsky, and Robert L. Byer. Optical parametric oscillator frequency tuning and control. *J. Opt. Soc. Am. B*, 8:646–667, 1991.

[24] J.E. Bjorkholm. Some spectral properties of doubly and singly resonant pulsed optical parametric oscillators. *Appl. Phys. Lett.*, 13:399–401, 1968.

[25] Smith R.G. Study of factors affecting performance of a continuously pumped doubly resonant optical parametric oscillator. *IEEE J. Quantum Electron.*, 9:530–540, 1973.

[26] M. Ebrahimzadeh, G. P. A. Malcolm, and A. I. Ferguson. Continuous-wave mode-locked optical parametric oscillator synchronously pumped by a diode-laser-pumped solid-state laser. *Opt. Lett.*, 17:183–185, 1992.

[27] D. Lee and N. C. Wong. Stabilization and tuning of a doubly resonant optical parametric oscillator. *J. Opt. Soc. Am. B*, 10:1659–1667, 1993.

[28] F. G. Colville, M. J. Padgett, and M. H. Dunn. Continuous-wave, dual-cavity, doubly resonant, optical parametric oscillator. *Appl.Phys. Lett.*, 64:1490–1492, 1994.

[29] L. E. Myers, R. C. Eckardt, M. M. Fejer, R. L. Byer, and W. R. Bosenberg. Multigrating quasi-phase-matched optical parametric oscillator in periodically poled $LiNbO_3$. *Opt. Lett.*, 21:591–593, 1996.

[30] L. E. Myers and W. R. Bosenberg. Periodically Poled Lithium Niobate and quasi-phase matched optically parametric oscillators. *IEEE J. Quantum Electron.*, 33:1663–1672, 1997.

[31] Martin M. Fejer, G.A. Magel, Dieter H. Jundt, and Robert L. Byer. Quasi-phase matched second harmonic generation: tuning and tolerances. *IEEE J. Quantum Electron.*, 28:2631–2653, 1992.

[32] Martin M. Fejer and W. R. Bosenberg. Periodically poled lithium niobate and quasi-phase matched optical parametric oscillators. *IEEE J. Quantum Electron.*, 33:1663–1672, 1997.

[33] D. Jundt. Temperature dependent Sellmeier equation for the index of refraction n_e, in congruent lithium niobate. *Opt.Lett.*, 22:1553–1555, 1997.

[34] I.D. Lindsay, B. Adhimoolam, P. Gross, M.E. Klein, and K.-J. Boller. 110 GHz rapid, continuous tuning from an optical parametric oscillator pumped by a fiber-amplified DBR diode laser. *Opt. Express*, 13:1234 – 1239, 2005.

[35] M. E. Klein, D.-H. Lee, J.-P. Meyn, K.-J. Boller, and R. Wallenstein. Singly resonant continuous-wave optical parametric oscillator pumped by a diode laser. *Opt. Lett.*, 24:1142–1144, 1999.

[36] M. E. Klein, D. H. Lee, and K. J. Boller J. P. Meyn, and R. Wallenstein. Singly resonant continuous-wave optical parametric oscillator pumped by a diode laser. *Opt. Lett.*, 24:1142–1144, 1999.

[37] Y. Tohmori, Y. Yoshikuni, H. Ishii, and Y. Kondo F. Kano, and T. Tamamura, and M. Yamamoto. Broad-range wavelength-tunable superstructure grating (SSG) DBR lasers. *IEEE J. Quantum Electron.*, 29:1817–1823, 1993.

[38] J. Rieger B. Borchert T. Wolf, S. Illek and M.-C. Amann. Tunable twin-guide (TTG) distributed feedback (DFB) laser with over 10 nm continuous tuning range. *Electron. Lett.*, 29:21242125, 1993.

[39] D. Wandt, M. Laschek, K. Przyklenk, A. Tünnermann, and H. Welling. External cavity laser diode with 40 nm continuous tuning range around 825 nm. *Optics. Communs*, 130:81–84, 1996.

[40] D. Marcuse. *Principles of optical fiber measurements.* New York, Academic Press, Inc., 1981. 368 p, 1981.

[41] E. Snitzer, H. Po, F. Hakimi, R. Tumminelli, and B. C. McCollum. Double clad, offset core nd fiber laser. *Optical Fiber Sensors Conference, New Orleans.*, page PD5, 1988.

[42] P. Even and D. Pureur. High-power double-clad fiber lasers: a review. *Proceedings of SPIE.*, 4638:1–12, 2002.

[43] V. Doya, O. Legrand, and F. Mortessagne. Optimised absorption in a chaotic double-clad fiber amplifier. *Opt. Lett.*, 26:872–874, 2001.

[44] M. J. Digonnet. *Rare earth doped fiber lasers and amplifiers*. Marcel Dekker, Inc. New York,, 1993.

[45] Paschotta, Rudiger, Johan Nilsson, Anne C. Tropper, and David C. Hanna. Ytterbium-doped fiber amplifiers. *IEEE J. Quantum Electron.*, 33:1049 – 1056, 1997.

[46] Pask H.M., Carman R.J., Hanna D.C., Tropper A.C., Mackechnie C.J., Barber P.R., and Dawes J.M. Ytterbium-doped silica fiber lasers: versatile sources for the $1-1.2\mu$m region. *IEEE J. Sel. Topics Quantum Electron.*, 1:2–13, 1995.

[47] P. Wessels and Carsten Fallnich. Polarization dependent gain in neodymium and ytterbium doped fiber amplifiers. *Opt. Express*, 11:530–534, 2003.

[48] A. Liem, J. Limpert, H. Zellmer, and A. Tunnermann. $100-W$ single-frequency master-oscillator fiber power amplifier. *Opt. Lett*, 28:1537 – 1539, 2003.

[49] Y. Jeong, J. Nilsson, J.K. Sahu, D.B.S. Soh, G. Alegria, P. Dupriez, C.A. Codemard, D.N. Payne, R. Horley, L.M.B. Hickey, L. Wanzcyk, C.E. Chryssou, J.A. Alvarez-Chavez, and P.W. Turner. Single-frequency, single-mode, plane-polarized ytterbium-doped fiber master oscillator power amplifier source with $264W$ of output power. *Opt. Lett*, 30:459 – 461, 2005.

[50] Y. Jeong, J. Sahu, D. Payne, and J. Nilsson. Ytterbium-doped large-core fiber laser with 1.36 kw continuous-wave output power. *Opt. Express*, 12:6088–6092, 2004.

[51] R. W. Boyd. *Non-linear optics*. Academic Press, San Diego, 1992.

[52] R. H. Stolen and C. Lin. Self phase modulation in silica optical fibers. *Phys. Rev. A*, 17:1448, 1978.

[53] M. N. Islam, L. F. Mollenauer, R. H. Stolen, J. R. Simpson, and H. T. Shang. Cross-phase modulation in optical fibers. *Opt. Lett*, 12:625–627, 1987.

[54] S. Song, C. T. Allen, K. R. Demarest, and R. Hui. Intensity-dependent phase-matching effects on four-wave mixing in optical fibers. *J. Lightw. Technol.*, 17:22852290, 1999.

[55] R. G. Smith. Optical power handling capacity of low loss optical fibers as determined by stimulated Raman and Brillouin scattering. *App. Phys. Lett.*, 21:2489–2494, 1972.

[56] R. W. Hellwarth. Third order optical susceptibilities of solids and liquids. *Prog.Quant.Electron.*, 4:1–68, 1977.

[57] Y. R. Shen. *Principles of non-linear optics*. Wiley, New York, 1984.

[58] R. H. Stolen, J. E. Bjorkholm, and A. Ashkin. Phase-matched three-wave mixing in silica fiber optical waveguides. *Appl. Phys. Lett.*, 24:308–310, 1974.

[59] R. H. Stolen, E. P. Ippen, and A. R. Tynes. Raman oscillation in glass optical waveguide. *App. Phys. Lett.*, 20:62–64, 1972.

[60] E.P. Ippen and R.H. Stolen. Stimulated Brillouin scattering in optical fibers. *App. Phys. Lett.*, 21:539–541, 1972.

[61] Govind P. Agarwal. *Non-linear fiber optics*. Optics and Photonics, Academic Press, 1993.

[62] N. A. Brilliant. Stimulated Brillouin scattering in double-clad fibers. *J. Opt. Soc. Am. B*, 19:2551–2558, 2002.

[63] M.F. Ferreira. Effect of stimulated Brillouin scattering on distributed fibre amplifiers. *Electron. Lett*, 30:40–42, 1994.

[64] C. N. Pannell, P. St. J. Russell, and T. P. Newson. Stimulated Brillouin scattering in optical fibers: the effects of optical amplification. *J. Opt. Soc. Am. B*, 10:684690, 1993.

[65] R. M. Shelby, M. D. Levenson, and P. W. Bayer. Guided acoustic-wave Brillouin scattering. *Phys. Rev. B*, 31:52445252, 1985.

[66] R. W. Boyd, Rzazewski. K, and P Narum. Noise initiation of stimulated Brillouin scattering. *Phys. Rev. A*, 42:5514–5521, 1990.

[67] J. Botineau, E. Picholle, and D. Bahloul. Effective stimulated Brillouin gain in singlemode optical fibres. *Electron. Lett.*, 23:2032–2034, 1995.

[68] N. Yoshizawa and T. Imai. Stimulated Brillouin scattering suppression by means of applying strain distribution to fiber with cabling. *IEEE J. Lightwave Technol.*, 11:1518–1522, 1993.

[69] J. Hansryd, F. Dross, M. Westlund, P. A. Andrekson, and S. N. Knudsen. Increase in the SBS threshold in a short highly nonlinear fiber by applying a temperature distribution. *IEEE J. Lightwave Technol.*, 19:1691–1697, 2001.

[70] V. I. Kovalev and R. G. Harrison. Suppression of stimulated Brillouin scattering in high-power single-frequency fiber amplifiers. *Opt.Lett.*, 31:161–163, 2006.

[71] I. Zawischa, K. Plamann, C. Fallnich, H. Welling, H. Zellmer, and A. Tunnermann. All-solid-state neodymium-based single-frequency master-oscillator fiber power-amplifier system emitting $5.5W$ of radiation at 1064 nm. *Opt. Lett*, 24:469–471, 1999.

[72] Guido Grosso and Anders Hook. Generation of short pulses by stimulated Brillouin scattering in optical fibers. *J. Opt. Soc. Am. B*, 10:2551–2558, 1993.

[73] S. Rae, I. Bennion, and M.J. Cardwell. New numerical model of stimulated Brillouin scattering in optical fibres with nonuniformity. *Opt. Commun.*, 123:611–616, 1996.

[74] R. V Johnson and J. H. Marburger. Relaxation oscillation in stimulated Raman and Brillouin scattering. *Phys. Rev. A*, 4:1175–1182, 1971.

[75] U. Motschmann K. Baumgartel and K. Sauer. Self-pulsing at stimulated scattering processes. *Opt. Commun.*, 123:51–53, 1984.

[76] A. L. Gaeta and R. W. Boyd. Stochastic dynamics of stimulated Brillouin scattering in an optical fiber. *Phys. Rev. A*, 44:32053209, 1991.

[77] Vincent Leceeuche, Bernard Segard, and Jaouad Zemmouri. On route to chaos in stimulated Brillouin scattering with feedback. *Opt. Commun.*, 172:335–345, 1999.

[78] R. G. Harrison, J. S. Uppal, A. Johnstone, and J. V. Moloney. Evidence of chaotic stimulated Brillouin scattering. *Phys. Rev. Lett.*, 65:167170, 1990.

[79] Robert G. Harrison Valeri I. Kovalev. The dynamics of a SBS fibre laser: the nature of periodic spiking at harmonics of the fundamental oscillation frequency. *Opt. Commun.*, 204:349354, 2002.

[80] J. P. Koplow, D. A. Kliner, and L. Goldberg. Single-mode operation of a coiled multimode fiber amplifier. *Opt. Lett.*, 25:442–444, 2000.

[81] A. Hirose, Y. Takushima, and T. Okoshi. Suppression of stimulated Brillouin scattering and Brillouin crosstalk by frequency-sweeping spread-spectrum scheme. *J. Opt. Commun.*, 12:82–85, 1991.

[82] R.H. Page, R.J. Beach, C.A. Ebbers, R.B. Wilcox, S.A. Payne, W.F. Krupke, C.C. Mitchell, A.D. Drobshoff, and D.F. Browning. High-resolution, near-diffraction-limited, tunable solid-state visible light source using sum frequency generation. *Conference on Lasers and Electro-Optics, Washington, D.C*, 39:17, 2000.

[83] B. Adhimoolam, M. E. Klein, C. J. Lee, P. Groß, I. D. Lindsay, and K.-J. Boller. Spectral shaping of a 10W diode laser-Yb-fiber amplifier system. *Rev. Sci. Instrum.*, 77:093101–1– 093101–4, 2006.

[84] R. M. Mueller. The Yb fiber laser for metastable ^3He optical pumping at *Jülich*. *Physica B*, 297:277–281, 2001.

[85] G. Tastevin M. Leduc and, P. J. Nacher and and E. Courtade. Kinetics of helium 3 laser optical pumping. *Hyperfine Interactions*, 127:443–449, 2000.

[86] G. Tastevin, S. Grot, E. Courtade, S. Bordais, and P.-J. Nacher. A broadband ytterbium-doped tunable fiber laser for 3He optical pumping at 1083 nm. *Appl. Phys. B*, 78:145–156, 2004.

[87] P.Tremblay, J. Beaubien, A. Michaud, and E. Cauchon. Enhancement of optical pumping efficiency by frequency-modulated lasers. *J. Opt. Soc. Am. B*, 9:15371542, 1992.

[88] S. Bordais, S. Grot, Y. Jaouen, P. Besnard, and M. Le Flohic. Double-clad 10-W Yb^{3+} fiber master oscillator power fiber amplifier for He^{3+} optical pumping. *Appl. Opt.*, 43:2168–2174, 2004.

[89] M. Elbel, C. Larat, P. J. Nacher, and M. Leduc. Optical pumping of helium-3 with a frequency-electromodulated laser. *J. Phys. France*, 51:39–46, 1990.

[90] S. V. Chernikov, J. R. Taylor, N. S. Platonov, V. P. Gapontsev, P. J. Nacher, G. Tastevin, M. Leduc, and M. J. Barlow. 1083 nm ytterbium doped fibre amplifier for optical pumping of helium. *Electronic. Lett*, 33:787–789, 1997.

[91] L. Hofmann, A. Klehr, F. Bugge, H. Wenzel, V. Smirnitski, J. Sebastian, and G. Erbert. 180mw dbr lasers with first-order grating in gaas emitting at 1062nm. *Electron. Lett.*, 36:534–535, 2000.

[92] K-H. Hasler, H. Wenzel, A. Klehr, and G. Erbert. Simulation of the generation of high-power pulses in the GHz range with three-section dbr lasers. *IEE Proc.-Optoelectron*, 149:152–160, 2002.

[93] A. Hirose, Y. Takushima, and T. Okoshi. Suppression of stimulated Brillouin scattering and Brillouin crosstalk by frequency-sweeping spread-spectrum scheme. *J.Opt.Commun.*, 12:82–, 1991.

[94] R. J. Webster. Spectral line profiles generated by deterministic frequency modulation. *IEEE transactions on signal processing.*, 39:1012–1017, 1991.

[95] M. Ito S. Kobayashi, Y. Yamamoto and T. Kimura. Direct frequency modulation in AlGaAs semiconductor lasers. *IEEE journal of Quant. Electron.*, 18:582–595, 1982.

[96] B. Adhimoolam, M.G. Hekelaar, P. Gross, I.D. Lindsay, and K.-J. Boller. Wavelength-tunable short-pulse diode-laser fiber-amplifier system around 1.06μm. *IEEE. Photon. Technol. Lett.*, 18:838– 840, 2006.

[97] J.-X. Cheng, A. Volkmer, L. D. Book, and X. S. Xie. An epi-detected coherent anti-Stokes Raman scattering (E-CARS) microscope with high spectral resolution and high sensitivity. *J. Phys. Chem. B*, 105:1277–1280, 2001.

[98] Andreas Zumbusch, Gary R. Holtom, and X. Sunney Xie. Three-dimensional vibrational imaging by coherent anti-Stokes Raman scattering. *Phys. Rev. Lett.*, 82:4142–4145, 1999.

[99] Eric O. Potma and X. S. Xie. Detection of single lipid bilayers with coherent anti-Stokes Raman scattering (CARS) microscopy. *J. Raman Spectrosc.*, 34:642–650, 2003.

[100] A. Robertson, M. E. Klein, M. A. Tremont, K.-J. Boller, and R. Wallenstein. $2.5GHz$ repetition rate singly resonant optical parametric oscillator synchronously pumped by a mode-locked diode oscillator amplifier system. *Opt. Lett.*, 25:657–659, 2000.

[101] S. Lecomte, R. Paschotta, S. Pawlik, B. Schmidt, K. Furusawa, A. Malinowski, D. J. Richardson, and U. Keller. Optical parametric oscillator with a pulse repetition rate of $39GHz$ and $2.1W$ signal average output power in the spectral region near $1.5\mu m$. *Opt. Lett.*, 30:290–292, 2005.

[102] P. Groß, M. E. Klein, T. Walde, K.-J. Boller, M. Auerbach, P. Weßels, and C. Fallnich. Fiber-laser-pumped continuous-wave singly resonant optical parametric oscillator. *Opt. Lett.*, 27:418–420, 2002.

[103] M. E. Klein, A. Robertson, M. A. Tremont, R. Wallenstein, and K.-J. Boller. Rapid infrared wavelength access with a picosecond PPLN OPO synchronously pumped by a mode-locked diode laser. *Appl. Phys. B*, 73:1–10, 2001.

[104] S. W. Corzine, J. E. Bowers, G. Przybylek, U. Koren, B. I. Miller, and C. E. Soccolich. Actively mode-locked GaInAsP laser with sub-picosecond output. *Appl. Phys. Lett*, 52:348–350, 1988.

[105] P. P. Vasil"ev. Ultrashort pulse generation in diode lasers. *Opt. Quantum Electron*, 24:801–824, 1992.

[106] A. Hideur, T. Chartier, M. Brunel, S. Louis, C. Özkul, and F. Sanchez. Generation of high energy femtosecond pulses from a side-pumped Yb-doped double-clad fiber laser. *Appl. Phys. Lett.*, 79:3389–3391, 2001.

[107] O. G. Okhotnikov, L. Gomes, N. Xiang, T. Jouhti, and A. B. Grudinin. Mode locked ytterbium fiber laser tunable in the $980 - 1070$ nm spectral range. *Opt. Lett.*, 28:1522–1524, 2003.

[108] A. Malinowski, A. Piper, J. H. V. Price, K. Furusawa, Y. Jeong, J. Nilsson, and D. J. Richardson. Ultrashort-pulse Yb^{3+}-fiber-based laser and amplifier system producing $25W$ average power. *Opt. Lett.*, 29:2073–2075, 2004.

[109] M. J. Brennan, A. J. Budz, B. J. Robinson, P. Mascher, and H. K. Haugen. Ultrashort optical pulse generation with a mode locked long wavelength $(1075 - 1085nm)$ InGaAs-GaAs semiconductor laser. *IEEE Photon. Technol. Lett.*, 16:1798–1780, 2004.

[110] A. Piper, A. Malinowski, B. C. Thomsen, D. J. Richardson, L. M. B. Hickey, and M. N. Zervas. $11.1W$ average power, 20 ps pulses at $1GHz$ repetition rate from a fiber-amplified gain switched 1.06 μm FabryPerot laser diode. *Conf. Lasers and Electro-Optics*, page CTuCC3, 2005.

[111] T. W. Hänsch. Repetetively pulsed tunable dye laser for high-resolution spectroscopy. *Appl. Opt.*, 11:895–898, 1972.

[112] D. Marcuse. Pulse distortion in single-mode fibers. 3: chirped pulses. *Appl. Opt.*, 20:3573–3579, 1981.

[113] A. S. Hou, R. S. Tucker, and G. Eisenstein. Pulse compression of an actively modelocked diode laser using linear dispersion in fiber. *IEEE Photon. Technol. Lett.*, 2:322–324, 1990.

[114] D. J. Richardson S. H. Yun, D. O. Culverhouse, and B. Y. Kim. Wavelength-swept fiber laser with frequency shifted feedback and resonantly swept intra-cavity acoustooptic tunable filter. *IEEE J. Select. Topic Quantum Electron.*, 3:1087–1096, 1997.

[115] P. F. Wysocki, M. J. F. Digonnet, and B. Y. Kim. Broad-spectrum, wavelength-swept, erbium-doped fiber laser at 1.55 μm. *Opt. Lett.*, 15:879881, 1990.

[116] Balaji Adhimoolam, Marvin E. Klein, Ian D. Lindsay, Petra Groß, Chris J. Lee, and Klaus-Jochen Boller. Widely and rapidly tunable semiconductor master oscillator-fiber amplifier around 1080nm. *submitted in IEEE Photon. Technol. Lett.*, 2006.

[117] S. R. Chinn, J. G. Fujimoto, and E. A. Swanson. Optical coherence tomography using a frequency-tunable optical source. *Opt. Lett.*, 22:340–342, 1997.

[118] B. Golubovic, B. E. Bouma, G. J. Tearney, and J. G. Fujimoto. Optical frequency domain reflectometry using rapid wavelength tuning of a Cr : forsterite laser. *Opt. Lett.*, 22:1704–1706, 1997.

[119] S. H. Yun, D. J. Richardson, and B. Y. Kim. Interrogation of fiber grating sensor arrays with a wavelength-swept fiber laser. *Opt. Lett.*, 23:843–845, 1998.

[120] P. Groß, B. Adhimoolam, M.E. Klein, I.D. Lindsay, K. Hsu, and K.-J. Boller. 9-Watt cw swept-wavelength diode-oscillator Yb-fiber-amplifier system. *Conference on Lasers and Electro-Optics*, CLEO/QELS and PhAST Technical Digest, 2006.